AN INTERCOMPARISON BETWEEN SIX WAVE RECORDERS AT NMI TOWER, CHRISTCHURCH BAY

J.A. CRABB, J.S. DRIVER, R.A. HAINE

REPORT NO. 154
1983

NATURAL ENVIRONMENT RESEARCH COUNCIL
INSTITUTE OF OCEANOGRAPHIC SCIENCES

INSTITUTE OF OCEANOGRAPHIC SCIENCES

Wormley, Godalming,
Surrey, GU8 5UB.
(0428 - 79 - 4141)

(Director: Dr. A.S. Laughton FRS)

Bidston Observatory,
Birkenhead,
Merseyside, L43 7RA.
(051 - 653 - 8633)

(Assistant Director: Dr. D.E. Cartwright)

Crossway,
Taunton,
Somerset, TA1 2DW.
(0823 - 86211)

(Assistant Director: M.J. Tucker)

When citing this document in a bibliography the reference should be given as follows:-

CRABB, J.A., DRIVER, J.S. & HAINE, R.A. 1983 An intercomparison between six wave recorders at NMI Tower, Christchurch Bay. *Institute of Oceanographic Sciences, Report,* No. 154, 74pp.

INSTITUTE OF OCEANOGRAPHIC SCIENCES

TAUNTON

An intercomparison between six wave recorders at NMI Tower, Christchurch Bay

by

J.A. CRABB, J.S. DRIVER & R.A. HAINE

I.O.S. Report No. 154

1983

This project was supported financially by the Department of Industry

An intercomparison between six wave recorders at NMI Tower, Christchurch Bay

1. SUMMARY

1.1 The report describes the field trial of six different types of wave recorder. The site chosen for the trial was the National Maritime Institute tower in Christchurch Bay on the south coast of England. The tower was in a reasonably exposed situation, it already had one wave recording system on the structure and two nearby, mains power was available and data could be transmitted to a shore base on an existing radio link. These permanent wave recorders comprised a Comex capacitance staff wave recorder mounted on one leg of the tower, and two buoys - a Datawell Waverider and an NBA Wavecrest - moored respectively about 50 m and 100 m from the tower in the sector to the south west. In addition to these and for the purpose of this experiment, an EMI laser was mounted on the structure and immediately below this, on the sea bed, was positioned a Simrad inverted echo sounder wave meter and an IOS pressure transducer. IOS installed these instruments with the help of NMI. The arrangement of the recorders is discussed in paragraph 3.3 of the report and figure 1 gives the positional details.

1.2 Analogue signals from the six instruments were filtered, scaled, digitised and transmitted to a shore base using the radio link. As a regular check on the data monitoring and transmission system integrity, calibration voltages were interleaved with the sensor signals before digitising into blocks. The shore base comprised a receiver/demodulater unit and a PDP-8 computer with multitrack tape deck and analogue monitoring facilities. The tapes were returned to the IOS Taunton Laboratory for validation checks and spectral analysis. The analysis system is described in section 5.

1.3 It was the intention to record continuous data sampled at a rate of 2 Hz for each channel of information (ie each instrument) for at least one month. As a consequence of some operational difficulties it was necessary to record for a period in excess of five weeks to ensure simultaneous recordings from all six instruments during several storm or strong wind events.

1.4 The data were stored on 7 track magnetic tape in a series of consecutive 2048 second records, during which all six sensors were sampled every half second. Every third record was extracted for validation checks, and records were declared valid or invalid depending upon the results.

1.5 The operational performance of each sensor is presented in a series of graphs

where the percentage of records rejected as invalid is plotted against the sea state parameters Hs and Tz. These parameters were derived from the Waverider results since this instrument was the most consistently reliable during the experiment.

1.6 In order to examine sensor responses a period of data recording was chosen which encompassed an adequate range of wind and therefore sea conditions. All data recorded in this period were validated and the 'good' records were spectrally analysed using a fast Fourier Transform routine. Manufacturer-quoted instrument frequency responses together with scaling factors derived from pre- and post-experiment calibrations were applied and moments of the corrected spectra calculated. Hs and Tz were computed from the moments using $Hs = 4\ M_o$ and $Tz = \sqrt{\frac{M_o}{M_2}}$ and were compared. The relationship between each instrument's response and that of the Waverider at a given frequency was determined and plotted. Additionally, in the case where three instruments were placed at precisely the same position on the tower, the Simrad inverted echo sounder and the IOS pressure sensor were compared against the EMI laser.

1.7 The comparisons of instrument response at different frequencies reveal apparent differences between some of the instruments. These results are discussed for individual sensors under separate headings; factors such as the applicability of the classical depth attenuation correction formula for the pressure signal and the effect of wire wetting on the capacitance staff are considered. The likelihood of the wave climate in the region of the tower being modified by reflections from the tower leg is examined as a possible explanation for some of the discrepancies noted.

2. INTRODUCTION

2.1 This work was carried out under a contract with the Department of Industry. The intention was to provide some indication of the comparative performance characteristics of some six wave measuring instruments, at least four of which were based on substantially different operating principles. Furthermore it was considered especially useful to examine the performance of some of the more recently introduced wave recording systems (the EMI laser and the Wavecrest buoy both come into this category) along with some of the more established systems such as the Datawell Waverider buoy.

2.2 It had been hoped that the measurement programme could be carried out in an exposed location in the North Sea but a suitable platform with the necessary facilities and accessibility could not be found. The National Maritime Institute tower in Christchurch Bay off the south coast of England is clearly in a less exposed situation with a mean water depth of 8.7 m but it offered a number of useful advantages which are discussed in section 3.1.

2.3 The original aim was to record wave data continuously from all six systems for a period of a winter month. In this way it was hoped to embrace at least one south or south westerly strong wind event as well as some calm and poor visibility conditions. In fact most of the equipment was installed on 5 February 1981 but, due to various operational difficulties, a month elapsed before all six systems were satisfactorily working together. Six uninterrupted sets of data were then recorded over the period 5 to 16 March 1981 and it was fortunate that, during this 11 days, several suitable wind events took place.

2.4 All instruments were calibrated under IOS direction and all the interface, digitising and recording equipment was designed and/or procured by IOS. The radio link and its associated modems were part of the standard NMI facilities. Much of the data handling electronics was purpose built. Descriptions of the wave recorders, their calibration, installation, and some comments on serviceability are made in section 3. Brief details of the tower and shore data handling system are provided in section 4, and expanded in appendix 7.3.

2.5 Data validation and analysis took place at IOS Taunton using some of the techniques developed for other IOS wave data collection projects and also using some of the experience gained from a previous experiment for comparing wave measuring instruments (ref 1). Section 5 describes these techniques.

2.6 The presentation of results in section 6 contains a series of separate discussions about the performance of each instrument and the numerical results are converted into a set of graphs to enable quick interpretation.

3. WAVE MEASUREMENT

3.1 Selection of Location

3.1.1 Some of the main considerations borne in mind during the selection of a

suitable site were as follows:

a) Reasonable exposure to wave activity encompassing locally generated as well as swell energy.
b) Good accessibility for instrument installation and maintenance.
c) Existence of reliable power supplies.
d) Presence of permanent staff to change tapes and monitor analogue signals on platform, or, alternatively, the facility to transmit data ashore in real time with an accessible shore station.
e) Availability of all facilities during winter months 1980/81.

In the event the site that could offer the best combination of features, the NMI Tower in Christchurch Bay, had the disadvantage of not being exposed to such severe conditions as a platform in the North Sea, nor was it large enough to accommodate staff for more that a few hours at a time. However, it possessed a reliable radio link together with a suitable shore station, and it offered as part of its normal equipment three wave recording systems. The purpose for which the tower was originally built was to provide a platform of suitable size to allow studies on such topics as wave loading, water particle motions and interactions between gravity type bases and the seabed. The wave height, water depth and structure dimensions bear a scale relationship of about 1 : 15 when compared to a platform in the Northern North Sea. Further information regarding the tower design and use are contained in references 2 and 3.

3.1.2 Of particular interest for this experiment was the tower's exposure to waves generated by local winds, especially where a reasonable fetch was involved. Fig 2 demonstrates that the site is well exposed to such winds between 155° and 250° with fetches typically in the range 75-200 miles. However, local topography (the existence of shingle and sand banks) meant that the greater part of the wave energy would be restricted to the approximate sector 170° to 230°, ignoring refraction effects. Swell energy radiating from storms in and beyond the western English Channel could reach the tower vicinity after some refraction caused by shallow areas south east of Hengistbury Head. A view of the tower from the south is shown in fig 3.

3.1.3 The 240v power supply on the tower was mains derived via a submarine cable link to the shore. Regular visits to the tower by NMI staff using small boats and Hovercraft meant that, weather conditions allowing, it was possible to visit

for servicing purposes as and when the need arose (although the presence of waves greater than about 1 m made landing difficult).

3.2 Description of Instruments

3.2.1 Waverider Buoy. The buoy used in this work was a standard 6000 series type with a hull diameter of 0.7 m. The buoy sensor was an accelerometer passively stabilised in the vertical plane for storm and swell wave frequencies. This produced a signal which after double integration was transmitted to the tower using the standard Datawell system with a carrier frequency of 26.990 MHz. A Warep receiver was used on the tower to receive this signal and an analogue output proportional to vertical displacement was fed to the interface unit. The internal chart recorder was disconnected throughout the experiment.

3.2.2 Wavecrest Buoy. This buoy is a relatively recent design and is intended to offer some advantages over the established Waverider system. Further details can be obtained from Ref 4. A single buoy of diameter 0.63 m was deployed. It embodied the same principle of operation as the Waverider ie an accelerometer passively stabilised in the vertical plane, but the design of the accelerometer and its suspension arrangements were quite different. The radio transmission system was a similar FM system but with a carrier frequency of 27.115 MHz. This signal was received on a separate Warep receiver at the tower and fed to the interface. Although the buoy mooring arrangements will be discussed in greater details in section 3.3, it is important to emphasise that whereas the Waverider incorporated the usual polar swivel mooring attachment at the base of the buoy the Wavecrest had an equatorial mount (one of the options offered by NBA). For purposes of making the most relevant comparison it would have been desirable also to use a polar mooring on the Wavecrest but such was not available at this site. Both buoys comprised part of the routine data collection equipment operated by NMI at this site.

3.2.3 Comex Wave Staff type WS2. The gauge was fitted by NMI to the South East side of the tower as a third means of collecting routine wave data. The sensor detected the sea surface elevation by means of the capacitance variation along a single, almost vertical, stainless steel wire coated with a layer of teflon. It is assumed that a type of bridge circuit was incorporated in the electronics package at the base of the staff but it has not been possible to verify this since the equipment is no longer manufactured by Comex and requests for circuits and

technical information have not been answered. The sensor electronics accepted a d c supply of 22-30 volt d c and returned an analogue signal proportional to sea surface elevation in the range 0-5 volts. There was no indication of the response of any low pass filters that might have been incorporated.

3.2.4 EMI Infra-red Wave Height Sensor. This equipment consisted of a small (190 mm x 290 mm diameter) sensor and electronics package fed by a remote two wire 12 to 18 volt d c power supply. It was mounted above the sea surface and 'looked' vertically downwards. As with the Comex staff the analogue return signal was proportional to sea surface elevation and lay in the range 0-5 v. The principle of operation involved the measurement of transit time of an infra red light pulse which was reflected back from the sea surface to the sensor receiving optics. The pulse repetition rate was about 16,000 per second and the beam width 1°. The incorporation of optical filters and electronic signal processing was intended to minimise the effect of sunlight and spurious reflections from rain and spray. No lens heater was fitted.

3.2.5 Simrad HW Wave Height Sensor. This is an echo sounder working in the inverted mode, and is unusual in that it uses a relatively high carrier frequency of 710 kHz to minimise errors in the pulse transit path caused by reflection from bubbles. In lower frequency echo sounding systems aeration effects can introduce substantial errors in measurement of the air/sea interface since bubble resonance frequencies may be similar to that of the carrier. The bubbles are usually concentrated at the surface but may also exist in layers at appreciable depth. The Simrad transducer was a ceramic device and transmitted pulses of 56 μS duration at a rate of 5 Hz. The beam width was quoted as being 2°. In addition to the transducer a transceiver unit was supplied and its purpose was to generate and transmit the acoustic pulse, and then to receive it and derive an analogue voltage from the transit time. The integrating circuitry, where conversion from a pulse transmit time to an analogue voltage took place, also incorporated error detection techniques designed to allow rejection of spurious signal returns. The output analogue voltage had a span of 0-10 v for a sea elevation of 0-30.5 m (0-100 ft).

3.2.6 IOS FM Pressure Recorder. The pressure transducer incorporates a diaphragm, the deflection of which by the applied pressure causes a change in separation distance of the two electrodes of a parallel plate capacitor. The variable capacitance thus produced is used to control the frequency of an oscillator.

The nominal frequency was 100 kHz. The FM signal was transmitted up a cable to an electronics unit where detection took place and an analogue signal of approximate sensitivity 0.4 v/m generated. Unlike the wave staff, laser and echo-sounder, the tidal or very low frequency component was removed by a high pass filter. The reason for this was that long term drift makes the transducer unsuitable for tidal and mean sea level measurements.

3.3 Siting and installation of instruments

3.3.1 Figure 1 shows the disposition of the instruments on and around the tower. The two buoys had originally been sited and deployed by NMI to the south west side of the tower. In this way they were fully exposed to the incident wave energy from the open sea. Therefore there was no reason to request any change of position for these. Since both moorings allowed considerable freedom of movement of the buoys over the sea surface then clearly a horizontal separation of 50 m or so in the mooring anchors (or nominal mooring positions) was essential.

3.3.2 The mooring configurations are shown in Fig 4.

3.3.3 The Comex staff, as already mentioned, was part of the tower equipment complement and had been fitted on the (removable) instrument support column to the south east side of the tower.

3.3.4 The comparison between the four tower supported instruments would have been aided if they could all have been installed at the same place. However the presence of the instrument support column and its associated transducers (particle velocity meters etc) made this impossible. The only other option was to mount the laser on the overhanging structure on the south west of the platform, and immediately below this, and on the platform support base, to fit the echo sounder and pressure transducer. These latter two sensors were located on a common mounting plate and their centres were separated by only 16 cms. The laser was immediately above and therefore all three instruments were measuring the sea surface within an area of less than 20 cms diameter. Figure 5 is a photograph of the two underwater sensors.

3.3.5 All receiving electronics for the wave recorders were situated in the platform general purpose room. Thus, in close proximity, there were two Warep receivers, a stabilised 18 v power supply for the laser, the Simrad transceiver,

and the FM pressure recorder electronics. The power to the Comex staff was provided by NMI and the output taken directly to the interface unit which was also mounted nearby. Figure 6 is a photograph of the equipment arrangement in the general purpose room.

3.4 Calibration of Instruments

3.4.1 The method of calibrating the Waverider and Wavecrest buoys was the well known one of rotating them through a circle of diameter 3 m whilst keeping them vertical. A series of rotational speeds were applied between the limits of approximately 0.025 and 0.25 Hz. In both cases the particular Warep receiver to be used in the experiment was tested with its buoy and the analogue output voltages measured between pins E and D of Plug A, the output from the Warep phase lock loop. This procedure was carried out both immediately before and after the experiment. The overall system sensitivies (buoy and receiver combined) expressed in terms of voltage output per metre, were shown to have changed as follows: Waverider +1.18%, Wavecrest +3.43%.

3.4.2 Both the laser and echo sounder were difficult to check for dynamic sensitivity. Static checks made before and after the experiment confirmed the manufacturer's quoted accuracies. The checks were made as follows:
Laser: A target was introduced at several range values between 1 and 50 metres and the output voltage compared with the distance measured by an accurate tape.
Echo sounder: The system was tested in a harbour with a large tidal range. The output was checked against a graduated staff at regular intervals throughout a tidal cycle. Salinity and temperature were also measured and compensated for.

3.4.3 Some attempt was made to check dynamic sensitivity and frequency response of the laser and echo sounder by using the IOS wave tank. The wave height and shape was recorded on a 16 mm cine camera filming through a window in the tank side. A metric scale was attached to the window. The non breaking waves generated by the wave maker had a maximum height of 30 cms and frequency span of 0.47 to 0.86 Hz and the mean depth of water was 1.83 m. Clearly this was a very restricted range but nonetheless gave some interesting results.

3.4.4. The laser output was very irregular and this was thought to be due to the difficulty in achieving good reflections of the beam from a smooth surface. Some improvement was evident if sawdust was introduced on the surface but the

results were too inconsistent to allow accurate dynamic calibration. However some indication of the effects of the internal low pass filter could be discerned, that is a gradual fall off in response amplitude with increase in wave frequency. As a separate exercise the beam width and symmetry was checked and found to be within specification.

3.4.5 The echo sounder also exhibited some noise in its output, ironically this was particularly obvious when sawdust was introduced to improve the laser operation since some particles drifted below the surface and caused spurious reflections. Four runs made at different wave frequencies within the 0.47 to 0.86 Hz range gave sufficiently consistent results to allow sensitivity calculations, and the resulting errors varied from -1.8% to +0.6% (the error is expressed as a percentage of the nominal sensitivity of 0.328 v/m or 0.1 v/ft). This was surprisingly good when consideration is taken of experimental error due to such factors as:

a) Lateral distortion of water surface between the point of pulse reflection and the air/water interface seen on the cine film
b) Meniscus effects on the tank window
c) Parallax errors
d) Interpolation between cine frames at times when the frame does not exactly coincide with the crest or trough (film speed 25 frames per second, therefore 1 frame = 0.04 secs)
e) Assymmetry of the wave shape, that is a tendency towards a cnoidal waveform.

3.4.6 The Comex wave staff was subjected to a static calibration in November 1980 by NMI (two months before commencement of the experiment). The calibration procedure was firstly to remove the staff and its support column, and then to immerse it in a series of steps whilst monitoring the output voltage. No dynamic calibration was made and neither was a post experiment static calibration carried out. The results of the 1980 calibration were presented by NMI as follows:

Sea elevation = $1.586 \times V_o - 3.000$ metres

where V_o = Comex output voltage.

Due to this equipment being a permanent part of the tower facilities, it was not possible to remove it to a wave tank or laboratory for dynamic checks.

3.4.7 Pressure transducers are most readily calibrated for their static response in a pressure vessel. The sensor used in this experiment was tested in the IOS

constant temperature pressure vessel at Bidston both before and after the experiment. The pressure/output frequency transfer function indicated an increase in transducer sensitivity of 0.61% over this period. The electronics unit was set up using a frequency modulated carrier generated by a precision oscillator, thus simulating a transducer under wave conditions. The change in gain of the electronics unit over the period of the experiment was found to be +1.0%. Once again it was not found possible to carry out a dynamic calibration of the sensor since, although pressure cycling test rigs do exist, the accuracy to which the pressure variation can be measured is inadequate.

3.4.8 During the experiment sea temperature and salinity were measured at several depths close to the laser/echo sounder/pressure sensor position. Little variation of either could be detected within the vertical column and the values over the course of the experiment were between 34.0‰ and 33.5‰ for the salinity and the temperature showed a variation from 6.4°C to 7.8°C. No particular trends were observed.

3.5 Operational reliability of instruments

3.5.1 Waverider Buoy. The buoy was deployed at the beginning of the experiment and worked reliably throughout. Similarly no troubles were experienced with the Warep receiver except for some radio interference on 25 February when maintenance work was being carried out in the vicinity of the tower.

3.5.2 Wavecrest Buoy. Deployment took place on 9 February but examination of analogue records at the shore station revealed intermittent long period oscillation of the mean line. The buoy was removed for examination on 10 February and then returned to NBA for repair. One printed circuit board was replaced (the navigation light drive circuitry) because of a faulty integrated circuit which may have affected the buoy power supplies, and the mean modulating frequency readjusted. A calibration check was made before re-deploying the buoy on 17 February. The buoy continued to exhibit mean line instabilities together with occasional large distrubances of the output signal. Discussions with NMI suggested that the most likely reason for these characteristics was lack of adequate damping in the equatorial mount. NMI say that the mounting system has now been modified so as to introduce more friction in the equatorial pivots (ref 5).

3.5.3 Comex Wave Staff. One day of data was lost between 10 and 11 February as

a result of work being carried out on the force sensors which were part of the same support assembly. On 16 February the whole support column was removed by NMI for major maintenance work on the force sensors and it was not re-fitted until 5 March. It was unfortunate that loss of data from the Comex occurred for so long during the operational phase of the experiment. Data return between 5 March and the end of the experiment on 16 March was high.

3.5.4 EMI Laser. No maintenance or repair work was necessary on this instrument during the experiment. On examination after removal very little salt deposit seemed to have accumulated on the optical surfaces. Comments about the possibility of loss of data due to fog are made in section 6.1.1.

3.5.5 Simrad ~~and~~ Echo Sounder. The front panel of the transceiver contained a variable gain control for adjusting the preamplifier sensitivity. Following installation it was found that the optimum position for the control was between 5 and 6 on the engraved scale. It remained in this position throughout the experiment. No maintenance work was required on the instrument; however some comments about data corruption are contained in section 6.1.2.

3.5.6 IOS Pressure Recorder. Some impulsive interference from the echo sounder was monitored on the transducer output but this did not appear on the signal feeding the interface unit. The instrument was reliable in operation and required no maintenance work. The transducer was free of corrosion and marine growth on recovery.

4. DATA TRANSMISSION AND RECORDING

4.1 System Description

Appendix III gives a full technical description of the data acquisition system but the following is a brief description.

Figure 7 shows a diagram of the overall system. The data acquisition system sequentially sampled all six wave recorders every half second. The signal from each wave recorder was buffered, scaled and fed to an analogue to digital converter (ADC) via a low pass anti-aliasing filter with a 3 dB cut-off at 1 Hz. The digital output from the ADC was stored in a memory before being transmitted to the shore station via a modem and radio frequency (RF) data link.

The shore station consisted of another RF data link and modem connected to a PDP-8 mini-computer acting as a data logger. This formatted the data before it was recorded on magnetic tape. It also output the data to a chart recorder via a display controller enabling a visiting operator to check that the system was working correctly.

4.2 Calibration

After the system was built and tested it was calibrated. Each of the anti-aliasing filters were dynamically calibrated by injecting a low frequency sine wave with a frequency range of 0.04 Hz to 3.0 Hz (25 seconds to 0.33 seconds period) and an amplitude equal to the expected maximum from its particular transducer. The system was then connected to the PDP-8 via a cable, instead of via the RF link and modems, and the whole system set running in a manual calibration mode. Readings were taken of the standard voltages on the various input cards and at various critical points in the system as well as at the output of the PDP-8. These calibrations were repeated at the end of the experiment and both sets of figures were then used when assessing the results as described later in this report.

5. DATA ANALYSIS

5.1 General Comments

The major requirements of a wave measuring instrument are that it should give a true record of the waves, and should do so over the complete range of conditions likely to be met in practice. Both aspects of performance have been addressed in the analysis of the data.

The reliability of the instruments has been determined by subjecting records sampled at regular intervals from throughout the data to a procedure designed to detect commonly occurring faults in wave records. An assessment of the ability of each device faithfully to measure waves has been made by a series of detailed intercomparisons of measured wave spectra. Only a small portion of the total data set has been used in this more detailed assessment.

5.2 Available Data

Wave data from the six sensors were recorded for a period of 37 days. The raw data, comprising more than thirteen hundred 2048 second records, resided on

sixteen magnetic tapes in the format described in appendix 7.3. A computer program was written to allow any number of 2048 second six channel records to be read, decoded and written to more conveniently handled disk files.

At times during the experiment some sensors were either not installed or had to be disconnected for various reasons. A separate record had been kept of such occurrences by engineers visiting the installation. In addition to the wave data, records of hourly mean wind speeds and direction had been obtained from the Meteorological Office for the nearby Hurn Airport. (Winds normally recorded on the tower installation were not reliable due to instrumentation failure.) Hourly records of visibility at Hurn and Portland Bill were also obtained.

5.3 Sensor Reliability Checks

All sixteen data tapes were accessed and every third six channel data record was retrieved for use in this section of the study. The time interval between the start of one retrieved record and the next was 111 minutes; 452 such records resulted.

Each 2048 second record returned by the individual sensors was inspected for faults. The computer program used for this purpose was one which has been used at IOS for some time in the validation of wave data routinely recorded at a number of Waverider stations. The tests which were applied to the data, check for the existence of the following faults:

1. Ten consecutive data points having equal value.
2. An interval between up-crossings of the record mean level greater than 25 seconds. This is applied only to the Waverider and Wavecrest buoys, and tests for the occurrence of mean line wander.
3. The mean zero crossing period less than the minimum value calculated on a maximum steepness assumption.
4. A difference in the magnitude of successive data points greater than the maximum value expected for the highest wave in the record.
5. Failure of the preceding test on two adjacent data points.
6. Magnitude of a data point exceeding four times the standard deviation of the record.
7. Failure of the preceding test on two adjacent data points.
8. An additional test was mounted which compared the recorded values of the calibration voltages, which precede and follow each data record, with the

nominal values.

The number of failures of each of these tests was noted for each data record. A record was declared valid or invalid after comparing the test failure score with a mask of allowable failures. This procedure has been monitored and refined during routine use and is known (with exceptions to be mentioned) to be capable of recognizing commonly occurring faults in measured wave records, and of assessing their overall quality and suitability for further processing. However, experience so far has been mainly confined to validating Waverider measurements and, therefore, the suitability of the tests for validating the records returned by the other instruments was confirmed by comparing the results for a large number of records with an experienced observer's assessment of the plotted traces.

All 452 records for each sensor were validated and, at the same time, the values of Hs and Tz for each record were calculated. The results of the validation procedure were compiled in a computer file which could be accessed to allow interpretation and presentation of the results. This file was edited and a note made (in the form of a coded flag) alongside each record where it was known that the sensor had been temporarily disconnected, or was otherwise not operational. Records so flagged were excluded from all further consideration, as were those records where test 8 indicated that calibration values had been incorrectly transmitted. This latter was taken as a possible indication of data-link transmission difficulties and as such was not allowed to influence the statistics of sensor performance. There were very few failures of this test.

The information on sensor performance throughout the experiment is presented in figures 11 to 15. The sea state parameters Hs and Tz, against which the results are plotted, are those derived from the Waverider measurements. The validation process showed this instrument to have been the most consistently reliable during the experiment (no validation test failures), and as such could be relied on to provide an indication of sea state. The use of the signal from this instrument (uncorrected for instrument response) as an approximate measure of sea state does not imply its acceptance as a standard.

The frequency distributions of the values of Hs and Tz observed during the experiment were compiled separately for each instrument, using only those observations which coincided with that sensor being operational. These distributions

were examined and the class widths adjusted to equalize the number of observations contained in each. Each class contains 50 (±1) observations. Figures 11 to 15 show for each instrument the percentage of the 50 observations in each class which were declared invalid. The first class in each distribution contained less than 50 observations and is drawn in a dashed line as a reminder. The number of observations actually contained is entered in parentheses alongside.

The general features of the results for each sensor are discussed in section 6.1.

5.4 Intercomparisons of Sensor Response

5.4.1 Preliminary processing: It was impracticable to make use of all the available data in this more detailed aspect of the study. Accordingly it was decided to base the intercomparisons on a shorter period of data during which an adequate range of conditions was encountered. Other conditions desirable for a meaningful comparison were also met during the selected period. Wind directions fell in an arc between 120° and 240°; waves from these directions approach the sensors without experiencing obstruction from the tower structure. All sensors were connected during this period and valid data returns were at a reasonable level.

The two field tapes containing the chosen data covered the period 5 to 9 March 1981. Both tapes were read completely and disk files formed of all 156 records which they contained.

Each record was examined using the validation procedure previously described; only those records qualifying as valid were used in the determination of sensor performance. In particular this means that all EMI laser records affected by fog, in so far as they could be recognized by the procedure outlined in section 6.1.1, have been excluded as invalid.

The spectrum of each 2048 second record was calculated using a Fast Fourier Transform routine. The complete record was transformed in one operation and no window was applied to the data. Each raw transform was then corrected for the known responses of the individual sensors as supplied by the manufacturer, and for the measured responses of the interface electronics. The spectra were scaled using the results of the calibration performed both before and after the experiment on the sensors and the interface electronics.

Moments of the corrected spectra were calculated according to

$$M_n = \frac{1}{T} \sum_{i=82}^{1229} E(fi).fi^n$$

where T is the record length in seconds.

The summation limits correspond to frequencies of 0.04 and 0.60 Hz.

The significant waveheight, Hs, and mean zero crossing period, Tz, were calculated from the moments using

$$Hs = 4\sqrt{M_o} \quad \text{and} \quad Tz = \sqrt{\frac{M_o}{M_2}}$$

The raw corrected spectrum was then smoothed by averaging over 20 adjacent harmonics to yield estimates with 40 degrees of freedom at 0.00976 Hz intervals. The smoothed spectra and their moments and derived quantities were written to disk file, along with the appropriate validation flag.

5.4.2 Comparison procedure: The purpose of this part of the study was to establish the relative response of the instruments at each frequency. With so many sensors it was impracticable to present a direct comparison of each instrument with all of the others. Instead, a reference sensor was chosen against which all the others were compared. The Waverider was chosen for this purpose. The choice of an instrument as a common reference point is not meant to imply its acceptance as a standard against which the other should be measured; it is simply a device to simplify the presentation of results. The consistently reliable operation of the Waverider during this experiment made it the natural choice for such a role.

The relationship between the response of each instrument and that of the Waverider at a given frequency was determined by performing a regression analysis on the population of measured values from each instrument at that frequency. The line which passed through the origin and which minimized the sum of squares of the perpendicular distances of the data points from it, was calculated. The 95% confidence limits on its slope were calculated (ie there is 95% probability that the true value of slope falls within these limits, which are approximately twice as wide as the standard error).

Figures 23 to 26 present the line slope and confidence interval for each frequency.

The energy at each frequency may be judged from the average spectrum of figure 18.

The relationships between the integrated height and period parameters, H_s and T_z, were determined in a similar manner. In this case the data points are plotted along with the regression lines in figures 19 to 22.

In an extension of the basic scheme in which all sensors were compared with the Waverider buoy, those sensors which were located at precisely the same position on the tower, ie the FM pressure recorder, the Simrad echo sounder and the EMI laser, have been compared. In this case the EMI laser was chosen as the reference instrument; records affected by fog were excluded. The Simrad and the EMI laser have been corrected for known instrumental responses and their comparison is straightforward. In the case of the FM pressure recorder, the major effect which must be corrected for is the hydrodynamic filtering effect of the water column. At the water depths experienced this effect is large at quite low frequencies. There has, however, been some discussion in the literature over the most appropriate form of correction to apply for this effect; in particular on the applicability of the classical formula. In view of this uncertainty and because of the large effect the choice of compensating function has on the results of any comparison, it was decided to plot the uncorrected data. In figure 27 the pressure recorder data, corrected only for electronic responses, are compared with the EMI laser. The form of the classical attenuation with depth equation is drawn superimposed on the data.

6. RESULTS

6.1 Sensor reliability results

EMI LASER

Visual inspection of traces returned by this instrument revealed occasional examples of obviously faulty operation. In these instances the instrument produced a low amplitude noise-dominated signal, illustrated in figure 16, which, because it displayed none of the faults tested for, was usually not recognized as faulty by the automatic validation procedure. However, values of Hs and Tz calculated for such records diverged wildly from those returned simultaneously by the other instruments. This behaviour was queried with the manufacturer who recognized it as characteristic of the instrument's response under foggy conditions (see section 6.2.1). The validation procedure for this instrument was therefore

supplemented by manually editing the validation file to reclassify as invalid all those records which displayed grossly anomalous Hs and Tz values, and which were recorded at times when atmospheric visibility (as recorded at Portland Bill) was less than approximately 300 metres.

During the assessment of the performance of the validation procedure on the signals returned by the other sensors, no further failure to recognize characteristically faulty behaviour was identified.

Figure 11 shows the failure rate for the EMI laser. Apart from the increased rate between 0.8 and 1.5 metres, within which most of the records affected by fog happened to occur, the distribution of failures appears independent of waveheight.

SIMRAD ECHO-SOUNDER

Figure 12 shows that the failure rate for this instrument was high, rising from around 30% at significant waveheights below 1 metre to almost 90% above 1.5 metres. Most failed records from this instrument exhibited large and sudden negative excursions of the trace (fig 17). It is suggested that such behaviour could be due to loss of the return signal under conditions where a proportion of waves are breaking and causing aeration of the water.

COMEX WAVE STAFF

Figure 13 shows the failure rate for this instrument to have been relatively low and with no marked dependence on waveheight. The performance of this instrument is discussed further in section 6.3.4.

FM PRESSURE SENSOR

This instrument returned very few faulty records, figure 14.

WAVECREST BUOY

As shown in figure 15 the failure rate was high and increased with increasing waveheight. Most failures were caused by the presence of mean line wander and occasional severe instability, as illustrated in figure 18.

WAVERIDER BUOY

No figure is presented for this instrument as no failures of the validation procedure occurred.

6.2 Manufacturers' Comments

Typical examples of faulty records returned by the EMI laser, the Simrad echo sounder and the NBA Wavecrest buoy were sent to the manufacturers of those instruments and their comments invited. The replies received are paraphrased below.

6.2.1 EMI Laser. "The anomalous effects evident on some of the time histories exhibited identical returns to those experienced with the instrument tested during the first series of trials at Rijkswaterstaat. This effect was traced to back scatter by fog. Subsequent modifications involving range gating and time varying gain have resulted in much improved performance in poor visibility conditions. Tests in a fog chamber indicate satisfactory operation down to 40 metres visibility. More recent trials of the modified instrument at Rijkswaterstaat during which thick fog was encountered on several occasions showed no repetition of the previous effects. It is understood that Rijkswaterstaat will be issuing an addendum to their original comparison report confirming the improved performance". IOS comment: this has been done, see references 8 and 9.

6.2.2 NBA Wavecrest. "The problems you have experienced do not particularly surprise us, bearing in mind the fact that the Wavecrest used in your trials was a prototype buoy and was not moored in a recommended manner. There is little doubt that the problems would not recur with a standard production buoy moored in the configuration specified by NBA.

The trace has been examined by our engineering staff who made the following comments:-

The sample of record supplied illustrates:-

a) a large and violent excursion from the mean, and,

b) a smaller amount of background zero wander.

The former was almost certainly caused by excessive pitch/roll angle. The Wavecrest suspension has end stops for pitch and roll and also for rotation. These stops prevent possible damage to the suspension due to excessive angular movement. It is important to ensure that the mooring configuration is such that it keeps these angles within reasonable limits. It is believed that the buoy in question was not moored in accordance with the configuration recommended by NBA (Controls) Ltd.

The second malfunction is a symptom of suspension wander. The buoy in question was an early prototype and problems were experienced with the ligament wires which were liable to produce suspension wander. Extensive development work has been carried out in this area as a result of which the performance has been vastly improved and the wander eliminated.

NBA has been carrying out a trials programme with a Wavecrest buoy in Mounts Bay, Cornwall since March this year (1982). During the early part of these trials it was found necessary to increase the mass of the ballast chain to improve the stability of the buoy. The data received since that time has shown only one type of malfunction ie under certain sea conditions the suspension pendulum very occasionally touches the rotational end stops causing an excursion in the data. However, only a small proportion of data has been spoiled in this way and the overall percentage is reasoned by us to be negligible when set against the advantages of a buoy which is very rugged and totally resistant to damage from spinning.

It should be emphasised that these trials have to date been undertaken using a standard diameter Wavecrest buoy which is about to be replaced by a large diameter unit. Indications are that the occasional excursion experienced with the standard buoy is virtually eliminated with the larger device."

6.2.3 No reply has been received to our letter and sample wave record sent to Simrad.

6.3 Intercomparison Results

In this report all sensors are compared to a common instrument to simplify the task of presenting the results. The main conclusion on sensor performance are drawn from a comparison of these relative responses. The agreement of one sensor with the chosen common instrument is not, on its own, given undue significance. In view, however, of the high reputation for reliability and accuracy which the Waverider has acquired over many years of use it must be admitted that agreement is not totally without significance. In this section the general picture emerging from the comparisons is described first and the performance of the individual sensors is then described in detail.

In general a high degree of correlation between the height and period measurements made with all instruments is apparent in the results of the comparisons shown in

figures 19 to 22. Differences exist, however, in the absolute heights ascribed to the waves and the source of these discrepancies is not obviously apparent. Static height calibrations of all instruments were conducted, and the results used in scaling the measured records before comparison. The dynamic calibrations performed to establish the instrumental response at frequencies other than DC were only satisfactory, however, for the two buoys. Consequently the nominal dynamic responses supplied by the manufacturers were used to correct the signals from the other sensors. It is possible that the discrepancies in scaling arose in part from this cause. It should also be noted that the Simrad echo-sounder and the EMI laser, which are both located on the tower, report Hs's in excess of those measured by the Waverider. There may thus be a real difference in wave climate between the two locations.

With the exception of the FM pressure sensor, the comparisons of spectral responses with the Waverider (Figs 23 to 26) divide into two groups of notably different character. The EMI laser and the Simrad echo sounder, which measured waves at the same spot beneath the south west arm of the tower, exhibit very similar relative responses. The Comex wavestaff on the south east arm of the tower and the Wavecrest, are also similar. The close agreement between the forms of the EMI and Simrad comparisons further strengthens the impression of a modified wave climate at that point. Wave reflections from the main tower leg are the most likely cause of this observation; the mechanism is discussed in section 6.3.2. The Comex staff, which is also located on the tower but in the vicinity of a second large pile, does not show this behaviour. In common with the Wavecrest it exhibits a tendency to progressive disagreement with the Waverider at higher frequencies. It may be that the hydrodynamic response of the Waverider, for which it was not possible to correct, is a contributory factor.

The results for individual instruments are discussed in the following sections.

6.3.1 FM PRESSURE UNIT As previously noted, the wave height data from this instrument require correction for the low pass filtering effect of the water column. In figure 27 the pressure recorder data, corrected only for electronic responses, are compared with the EMI laser. It should be noted that the results presented are average responses over a period of four days. The effect of the variation of tidal height during this period on the degree of filtering experienced by the pressure recorder thus manifests itself as scatter in the results. The confidence

limits, although reasonably narrow, are thus wider than they would have been had the mean water level remained constant throughout.

The classical formula for attenuation with depth has been plotted and is shown superimposed on the relative response data. The data might be expected to follow this curve if both instruments recorded otherwise undistorted wave heights. Agreement is quite close at frequencies below 0.28 Hz, above this point the pressure recorder returns values greatly in excess of those to be expected on the theory alone.

Several mechanisms which might account for this excess of high frequency energy were examined, and their effects compared with the observed values. The average spectrum recorded by the pressure recorder is shown in figure 28.

The spectral density in the elemental frequency band centred on 0.50 Hz is $1.53 \times 10^{-4} m^2/Hz$; implying a variance in this band of $1.49 \times 10^{-6} m^2$.

The contribution to this variance by each of the mechanisms considered is listed below; the details are described in appendix 1.

Signal expected from attenuated surface wave	$8.4 \times 10^{-11} m^2$
Quantization error, that is noise due to discrete sampling of the signal	$3.3 \times 10^{-8} m^2$
Leakage from other regions of the spectrum	$6.0 \times 10^{-8} m^2$
Presence of a standing wave component in the surface wavefield and the consequent appearance of a pressure component which does not attenuate with depth	$2.4 \times 10^{-10} m^2$
Electronic noise in the sensor and interface circuits (measured in the laboratory)	$1 \times 10^{-8} m^2$

Although the sources investigated do not appear to account for the observed signal, it should be noted that the equipment was operating in an electronically noisy environment which it was not possible to simulate fully in the laboratory. It is thus possible that the excess signal recorded by the pressure unit at high frequency was largely electronic noise. It may, however, be that the high frequency signal was induced by the surface waves. The inadequacy of the classical formula in describing the observed attentuation with depth could then be due to the fact that some of the high frequency energy is associated not with

independantly propogating surface waves, but derives from a non-sinusoidal surface profile. Under these circumstances the linear superposition assumption of the classical theory would be violated and a departure from the observations expected.

Figure 27 also reveals significant disagreement between the pressure recorder and the EMI laser at low frequencies where they might be expected to agree closely. It is clear from this figure that correcting the pressure recorder spectrum by the classical formula and then calculating Hs by summing over the whole frequency range, would not produce values which agreed with those reported by the laser. A common approach to the correction of pressure data is to calculate a single characteristic period, usually Tz, and use this to scale the attenuation with depth formula; the choice being made from the classical or Draper (ref 10) formulae. Agreement between wave heights calculated in this way, and those measured by the EMI laser was assessed by reduced major axis regression analysis. Both formulae gave correlation coefficients in excess of 0.95, the line slope in the classical case was 0.82 and for the Draper formula 0.92. Thus, in both cases the corrected pressure measurements underestimated the surface wave heights.

6.3.2 EMI LASER A plot of the significant wave heights recorded simultaneously by the EMI laser and the Waverider (Fig 19) exhibits a linear relationship with a high degree of correlation ($r = 0.97$). There is however, a 6% discrepancy in apparent scaling. In view of the evidence below for a somewhat modified wave climate at this point this discrepancy is not regarded as significant.

The comparison of spectral response with that of the Waverider (Fig 23) differs markedly from unity. A very similar form of relative response is found for the Simrad echo sounder and leads to the hypothesis that a real difference in the local wave climate, rather than an instrumental artifact, is being measured at this point. A possible mechanism of climate modification is that whereby, at each frequency, waves reflected or diffracted by the tower leg combine with the incoming waves to set up a standing wave pattern. The position of the transducer in the standing wave determines the apparent response at that frequency. If the measuring position coincides with a standing wave crest the apparent response is increased by the reflected wave amplitude, and correspondingly reduced at a trough. A simple model incorporating the tower geometry has been used to determine the approximate response; the resulting curve is shown superimposed on the spectral response data in figure 29. It can be seen that, whilst by no means perfectly

describing the observed behaviour, some of the broad features are reproduced. The similarity between the curves is sufficient to indicate that the presence of reflected waves in the vicinity of the tower is largely responsible for the apparent discrepency between the tower mounted EMI laser and the Waverider which measures the distant undisturbed wave field.

6.3.3 SIMRAD ECHO SOUNDER Significant wave heights recorded by the Simrad (Fig 20) exceed those measured by the Waverider by 17%. More significantly, they exceed the significant wave heights recorded at the same spot by the EMI laser by 8%. (Fig 30)

The comparison of spectral response with the Waverider is similar in form to that of the same comparison for the EMI laser; confidence intervals are wider however, probably as a consequence of the reduced number of valid observations. Direct comparison with the EMI laser (Fig 31) shows an apparent disagreement in scaling across the frequency range with an additional sharp rise in the apparent response at low frequencies. This latter observation should probably be interpreted as faulty behaviour in the Simrad as the laser agrees well with the Waverider at these frequencies. It could be that the behaviour which caused a large number of Simrad records to be rejected occurs in a less severe form in the records used in the comparison, and is responsible in part for the discrepancy.

6.3.4 COMEX WAVE STAFF Comparison of significant wave height against the Waverider (Fig 21) reveals behaviour not exhibited by the other instruments; the data are not well described by a line passing through the origin. The best fit line (Fig 32) indicates an offset of -0.27 m in the wave staff response. A similar form of behaviour is apparent in the comparison of significant wave height with the tower mounted EMI laser (Fig 34).

Relevant to this behaviour is the observation of a characteristic form of distortion found in many of the wave staff traces. An example is illustrated in figure 33, which also shows a portion of the trace from the EMI laser for comparison. Although the instruments were not located at the same point, some correlation between waves is apparent. The Comex trace generally fails to follow wave troughs to their full depth. This observation is consistent with a known phenomenon in which the falling water surface wets the capacitance wire leaving behind a thin film of water extending up the wire above the true water level. The true extent

of the trough is thus not registered as the capacitance between the sea water and the inner conductor remains artifically high. This same phenomenon could also account for the offset in the wave height comparison as, once wetted, the wire fails to record waves which are not high enough to encroach on the dry portion of wire.

The spectral response relative to the Waverider (Fig 25) is devoid of remarkable features but tends steadily to lower values at higher frequencies. Wetting would again account for this, as it may be supposed that the wire drains at a fixed rate and is thus unable to clear fully in the short interval between successive high frequency waves.

A further feature of the relative spectral response is its dissimilarity to that exhibited by the other tower mounted instruments. The tower plan shows a 0.48 m diameter pile close to the capacitance wire and its presence may be responsible for the difference. The average direction of wave approach during the period of detailed comparison was such that strong wave reflections in the direction of the staff were unlikely, and this may be a further reason for the different response.

6.3.5 WAVE CREST The significant wave heights and mean zero crossing periods returned by the Wavecrest are in close agreement with the Waverider (Fig 22).

The relative frequency response (Fig 26) shows a tendency to decrease with increasing frequency. It should be noted that the tendency to mean line wander exhibited by the Wavecrest may, to some extent, contaminate some of the records used in the comparison.

In view of the non-standard nature of the Wavecrest mooring supplied, a further experiment to compare the Wavecrest and Waverider buoys has been conducted off the South coast of England close to the Eddystone Light. In this case the mooring with a polar mount was used. Two examples of the Wavecrest buoy were deployed in succession during the winter 1981/82 and both failed due to tangling of the fine ligament wires which connect to the accelerometer. However, some acceptable wave records were obtained from the second buoy and compared with the Waverider. The interpretation of the comparisons has not proved to be straight forward and there is some evidence that wave refraction in the vicinity of the lighthouse may have affected the waves differently at the two sites. This experiment is to be re-

ported fully in a separate document.

7. APPENDICES

7.1 Appendix 1

Calculation of contributions to the average FM pressure recorder spectrum at high frequencies

A number of mechanisms have been identified which could possibly contribute significant signal variance at high frequency. The variance contributed to the spectral band centred on 0.5 Hz is calculated for each mechanism in turn.

7.1.1 Attenuated wave signal. Assuming that the EMI laser accurately records the surface wave amplitude in the frequency band being considered, the expected contribution to the pressure signal may be calculated using the classical attenuation with depth formula. The average depth of the water is 8.7 m and the pressure sensor is located 1.4 m above the bed. Classical theory gives the following as the factor by which the pressure fluctuation due to a surface wave with wave number, k , is attenuated with depth, z , in water of depth h .

$$G = \frac{\cosh(k(h-z))}{\cosh(kh)}$$

The spectral intensity in a given frequency band is thus reduced by a factor G^2 which, evaluated at 0.5 Hz, is

$$G^2 = 3.9 \times 10^{-7}$$

The surface spectral intensity at 0.5 Hz recorded by the EMI laser is 2.2×10^{-2} m^2/Hz, implying a variance in the band of $2.15 \times 10^{-4} m^2$. The expected variance in the same band as recorded by the pressure recorder is thus

$$= 2.15 \times 10^{-4}.G^2 = 8.4 \times 10^{-11} m^2$$

This compares with a variance of $1.49 \times 10^{-6} m^2$ actually recorded.

7.1.2 Quantization error. The wave sensor signal is rendered into digital form by determining which of a large number of discrete voltage levels is closest to the signal level at the moment of sampling.

If the interval between discrete levels is Δx then the variance of the error due

to the signal level approximation implicit in the above procedure is (from standard texts):

$$V = \frac{\Delta^2 x}{12}$$

In the present application the equivalent digitizing increment is 0.00634 metres giving rise to a total error variance of $3.35 \times 10^{-6} m^2$.

Assuming the noise spectrum to be white, the contribution to each of the 102 spectral bands is

$$Ve = \frac{3.35 \times 10^{-6}}{102} = 3.28 \times 10^{-8} m^2$$

7.1.3 Leakage from other regions of the spectrum. The Fourier transformation of a data record of finite length results in the total energy being distributed among a number of harmonic components. If the data record contains energy at a frequency not a harmonic of the record length, then some of this energy is attributed to harmonics removed in frequency from that of the component sinusoid. The amount of energy leaked in this manner is quantifiable, but to calculate the amount of energy leaked to a given component from all other components in a spectrum of arbitrary shape is tedious. In this case, the degree of leakage has been approximately ascertained by calculating the spectrum of a time series constructed by adding a number of sinusoids with frequencies which cover the most energetic region of the measured spectrum. The sinusoids had equal amplitude and random phase. The amount of energy occurring at 0.5 Hz, which is well outside the range of frequencies contained in the time series, was determined and expressed as a fraction of the energy at the spectral peak. The energy at the peak of the FM pressure unit spectrum was reduced by this same fraction to predict the amount of leaked energy at 0.5 Hz.

The variance of the signal in the band at 0.5 Hz was estimated to be $6 \times 10^{-8} m^2$.

7.1.4 Non-attenuating pressure component. The expression for the pressure, , at a point in the fluid beneath a standing wave (Ref 1) contains a term which does not attenuate with depth. Its magnitude is

$$\frac{p}{\rho g} = \frac{\pi H^2}{4L} \cdot \tanh\left(\frac{2\pi h}{L}\right) \cdot \cos\left(\frac{4\pi t}{T}\right)$$

where h is the water depth

L is the standing wave length

H is the standing wave height

To determine the variance in the elemental frequency band at 0.5 Hz from this source, the height of the standing wave caused by partial reflection of surface waves with a frequency of 0.25 Hz must be estimated. It is shown in reference 12 that the reflection coefficient, ie the ratio of incident to reflected amplitudes, at this frequency is approximately 0.095. The rms amplitude of the incident wave in this band (as measured by the Waverider) is 0.068 m, giving rise to a standing wave of height

$$H = 4 \times 0.068 \times 0.095 = 0.026 \text{ m}$$

with length $L = 23.8$ m (for water depth = 8.7 m)
giving from (1)

$$\frac{p}{\rho g} = 2.19 \times 10^{-5} \text{m}$$

The variance of a signal of this amplitude is

$$V = 2.39 \times 10^{-10} \text{m}^2$$

7.2 Appendix 2

Modification of local wave climate by wave reflection

The approximate effect of the tower on the wave climate at the tip of the south west arm is calculated using a simple model incorporating the average situation geometry. In particular it is assumed that the mean wave direction is the same as the mean wind direction. This assumption is reasonable at high wave frequency and it is these waves which are reflected most strongly by the structure. All waves are assumed to approach from the mean wave direction. Refer to figure 35 for these calculations.

An incident wave of amplitude a, and wave number k_1, is partially reflected from the tower leg. The reflected component in the directing of the sensor has amplitude ar, where r is the amplitude reflection coefficient. The incident wave number resolved in the direction of the sensor is $k_2 = k_1 \cos \phi$

Adding the incident and reflected waves in order to determine the surface behaviour at the sensor we have

$$\eta = a\cos(k_2x+\sigma t) + ar\cos(k_1x-\sigma t)$$

$$= a\cos k_2.\cos\sigma t - a\sin k_2 x.\sin\sigma t + ar\cos k_1x.\cos\sigma t + ar\sin k_1.\sin\sigma t$$

$$= a(\cos k_2 x + r\cos k_1 x)\cos\sigma t + a(r\sin k_1 x - \sin k_2 x)\sin\sigma t$$

$$= A\cos\sigma t + B\sin\sigma t$$

The amplitude of the equivalent single sinusoid is $C = \sqrt{A^2+B^2}$ thus

$$C = a^2\cos^2 k_2x + a^2r^2\cos^2 k_1x + 2a^2r\cos k_2x.\cos k_1x + a^2\sin^2 k_2x + a^2r^2\sin^2 k_1x - 2a^2r\sin k_2x.\sin k_1x$$

$$= a^2 + a^2r^2 + 2a^2r(\cos k_2x.\cos k_1x - \sin k_2x.\sin k_1x)$$

$$= a^2 + a^2r^2 + 2a^2r\cos(k_1+k_2)x$$

The amplitude reflection coefficient r has been determined by Longuet-Higgins and Cartwright (Ref 12) as a function of wave number, cylinder geometry and angle of reflection. A look up table of r for each wave number was compiled from reference 12 for the geometry detailed in the previous diagram. At each wave number the ratio of the spectral intensities of the local and distant (incident) waves is C^2/a^2. These ratios have been calculated using (1) and are plotted in figure 29.

7.3 Appendix 3

A Technical Description of the Data Acquisition System

7.3.1 System Description. Figure 7 shows a diagram of the overall system. The data acquisition system sequentialy sampled the wave signal from each of the six wave recorders every half second, taking about 100 microseconds for each channel. The data was stored in a first in first out (FIFO) register. The controller then output data from the FIFO to a universal asynchronous receiver transmitter (UART). Each channel sample consisted of 10 bits + 1 sign bit and 3 bits for channel identification. This 14 bit word was split into two 7 bit

words each being sent in turn, via the UART and line drivers where they were converted to RS232/V24 format, to the modem and RF data link. There was no redundancy built into this method of transmission for two reasons. The first was that the data link was only capable of transmitting at 300 baud (300 bits per second or 30 characters per second) and the data were being collected at rate of 240 baud (24 characters per second) leaving only 3 characters worth of time to transmit any redundant characters. The second was that it was felt that since the transmission path was very short (5 miles, and line of sight) the data would be valid at all times except when the transmitter was down with some major fault.

7.3.2 The shore station consisted of a radio frequency transmitter/receiver, a modem and a PDP-8 mini-computer acting as a data logger. The PDP-8 carried out a number of tasks; it formatted the data for recording on a 7-track industry standard ½ inch magnetic tape deck; it also output the data to a display controller.

7.3.3 Tower Data Acquisition System. Figure 8 shows a block diagram of the data acquisition system installed on the tower.

7.3.4 Input/Filter/Amplifier Board. Each board contained an anti-aliasing filter and amplifier, four reference voltage sources and five analogue switches. Logic controls were fed to each to switch the wave signals and reference voltages in the required sequence. The cards were identical except for the different values of reference voltages, offset voltages and amplifier gains required for the individual sensors.

The anti-aliasing filter was a low pass filter with a -3 dB cut-off at 1 second. The wave signal was fed to the inverting filter input and a dc offset voltage was applied to the non-inverting input. This offset voltage was different for each wave recorder and was adjusted so that the wave signal at the output of the filter was symmetrical about zero. The output from the filter was then fed to an inverting amplifier which increased the signal amplitude such that the maximum expected wave signal was equal to the input range of the ADC, ±10V. When the control unit required a signal from a certain wave recorder it transmitted a control signal and the particular wave signal was then sent along the analogue bus, via an analogue gate, directly to the ADC.

When set to calibrate mode, four set voltages within the range of the wave signals were switched in turn into the signal path instead of the wave signal to provide some indication of the performance of the system as a whole during the running of the experiment.

7.3.5 ADC Board. The board contained the ADC and FIFO registers for storing the ADC output and channel identifiers. The ADC was permanently connected to the analogue bus. The controller switched the required input amplifier to it in the correct sequence followed by a convert pulse to initiate conversion. The 12 bit conversion took 25 microseconds to complete, of which only 11 bits were used. The controller checked the status of the ADC end of conversion (EOC) line. When it was low the digital word was available on the output lines and presented to the input of the FIFO. At the same time each EOC was counted and was also presented to the FIFO to give channel identity. The controller then transmitted a pulse to shift the data into the FIFO. This sequence was repeated for each of the six wave recorders. When the FIFO had all six channels of data the controller started to send data to the UART.

7.3.6 Control Card. The purpose of the control card and its program was to sequence the operations in the system and to test the status of various status lines. The heart of the system was a Motrola MC14500B single chip, 1 bit static CMOS processor. A full description of the device can be found in reference 7. The processor takes the form of a 16 pin dual-in-line package and features 16 four bit instructions. These instructions perform logical operations on data appearing on a one bit bi-directional data line and also data in a one bit accumulating register within the processor. All operations were performed at the bit level. To enable the MC14500B to operate, six additional components had to be added to form a minimum system as shown in the block diagram in figure 9. These were:

Memory in the form of EPROM erasable programmable read only memory (EPROM). Here the program steps were stored, together with individual instructions and addresses of input and output ports.

A program counter, one that was synchronous, able to count up and down and be preset. This was used to step the machine through the sequence of instructions.

Input ports and output ports, each individually selected by the machine from information contained in memory.

A latch and full adder to enable the ICU to perform the instruction JUMP .-3

The MC14500B had a built in clock whose frequency was determined by a resistor. The program was stored in an EPROM type TMS2516 (2k*8). The counter was formed by two 4516 binary up/down counters. The system was built with eight input ports provided by a 4512, and an 8 channel data selector of which only 4 channels were used. The output ports were provided by two 4099, 8 bit addressable latches.

As can be seen this is not a conventional processor since all functions have to be hard wired. But in the form so far described it does operate on the principle of a stored program processor. Each stored command instructs the processor to perform one of sixteen operations. The system "fetches" a command on the positive going edge of a clock pulse, and then "executes" the command on the negative going edge. After executing the command the program counter is incremented on the next positive going edge and the next sequential command is fetched from memory and executed on the next negative going edge of the clock. This means it has a looping structure, it will follow through a program stored in EPROM but is unable to carry out any jumping or subroutines. However for most control applications, it may be an advantage to have a control structure with branching. Jumping and subroutines can reduce execution time and reduce software complexity.

On power up, a high level reset the MC14500B until the power supply had stabilised. It also cleared the input port latches, reset the program counter to the start address OOH and held the clock in the MC14500B in a high state. When the reset went low the oscillator started by going low and the counter output OOH appeared at the address input of the EPROM and was decoded. The output from the EPROM was split into two. The four least significant bits were fed to the input and output ports as addresses and the four most significant bits were fed to the MC14500B to be decoded into one of sixteen instructions on the next negative edge of the clock. On the next and subsequent clock pulses the process was repeated.

A simple routine incorporating jumping and conditional branching was implemented to enable the processor to test the status of a line without resorting to a long loop. The hardware required for the jump was suitable for testing all status lines. The JUMP .-3 instruction was implemented in the following manner: the output from the program counter was fed to the full adder as well as to the EPROM, where it was added to -3. This was then stored in the latch on the positive edge of the clock. If that current instruction was JUMP .-3, a pulse appeared on the JUMP pin of the ICU and the program counter was preset with the data from the latch.

7.3.7 UART Board. The board consisted of a UART, line drivers, line receivers and control port decoders. A data word appearing on the parallel data bus was loaded and transmitted in serial form. The controller arranged the correct sequencing of unloading the FIFO and loading the UART for transmission in RS232/V24 standard by the modem and the RF transmitter.

The modem and RF amplifier were provided as standard equipment on the tower, of which one duplex channel was used, and as such will not be described.

7.3.8 Shore System. The block diagram (Fig 7) shows the configuration of the shore system and figure 10 shows a photograph of the system. The shore system consisted of a PDP-8 mini-computer together with a dual floppy disc drive, a 7-track industry standard tape desk and a Silent 700 terminal. Also included was a display controller and precision chart recorder. The data were received on shore by the PDP-8 acting as a data logger via an RF transmitter/receiver and modem. The PDP-8 formatted the data and this included preceding each record with header information before it was sent to magnetic tape. The data output to the tape was also sent to the display controller. This carried out two functions: the first was to display, via a series of lights, a channel number and data in binary form: the second was to transmit the same data in analogue form by passing it through a digital to analogue converter (DAC) to a precision chart recorder, the channel number in question being selected by a switch. Both these displays enabled a visiting operator to take a "quick look" at the data and check that the system was working correctly. Finally there was a Silent 700 printer connected to the PDP-8 which gave out status information about the recording sequence, time, number of records and number of blocks recorded on the tape deck.

7.3.9 The PDP-8 controlled the time at which records were taken, the length of record, the header information and the format of the data on tape. It was also to control the operation of the system on the tower by starting and stopping the stream of data from the tower and by initiating internal calibrations.

A record on tape consisted of 4096 readings from each of the six wave recorders, each taken at half second intervals. Each record was made up of a number of blocks of data and each block consisted of 4096 words or 2048 readings (2 words to the reading and 1 reading per channel).

At the beginning of each record there was header information taking the form:

```
NOO*@@@@*@@@@*@@@@*@@@@*@@@@*
     ^    ^    ^    ^    ^
     1    2    3    4    5
```

where 1 is the day number

2 is the time in hours

3 is the time in minutes

The time was in GMT and represented the time when the header was recorded.

4 was the block number. This was the number of the blocks recorded on tape up to that time.

5 was the record number. This was the number of the record about to be recorded.

There then followed a calibration. This involved disconnecting the signal from the wave recorders and injecting five different known d c voltages through the tower electronics. These calibration voltages were sampled five times in the usual manner. This procedure was controlled by the PDP-8 and recorded on to the magnetic tape. There then followed the 4096 readings from each channel at half second intervals. This was equivalent to 34 minutes 8 seconds of data. This was followed by another header NOO* etc; and finally another calibration. The whole sequence then started again unless the operator indicated to the PDP-8, via the control switches on the front panel, that a manual calibration or tape change was required.

8. FIGURES

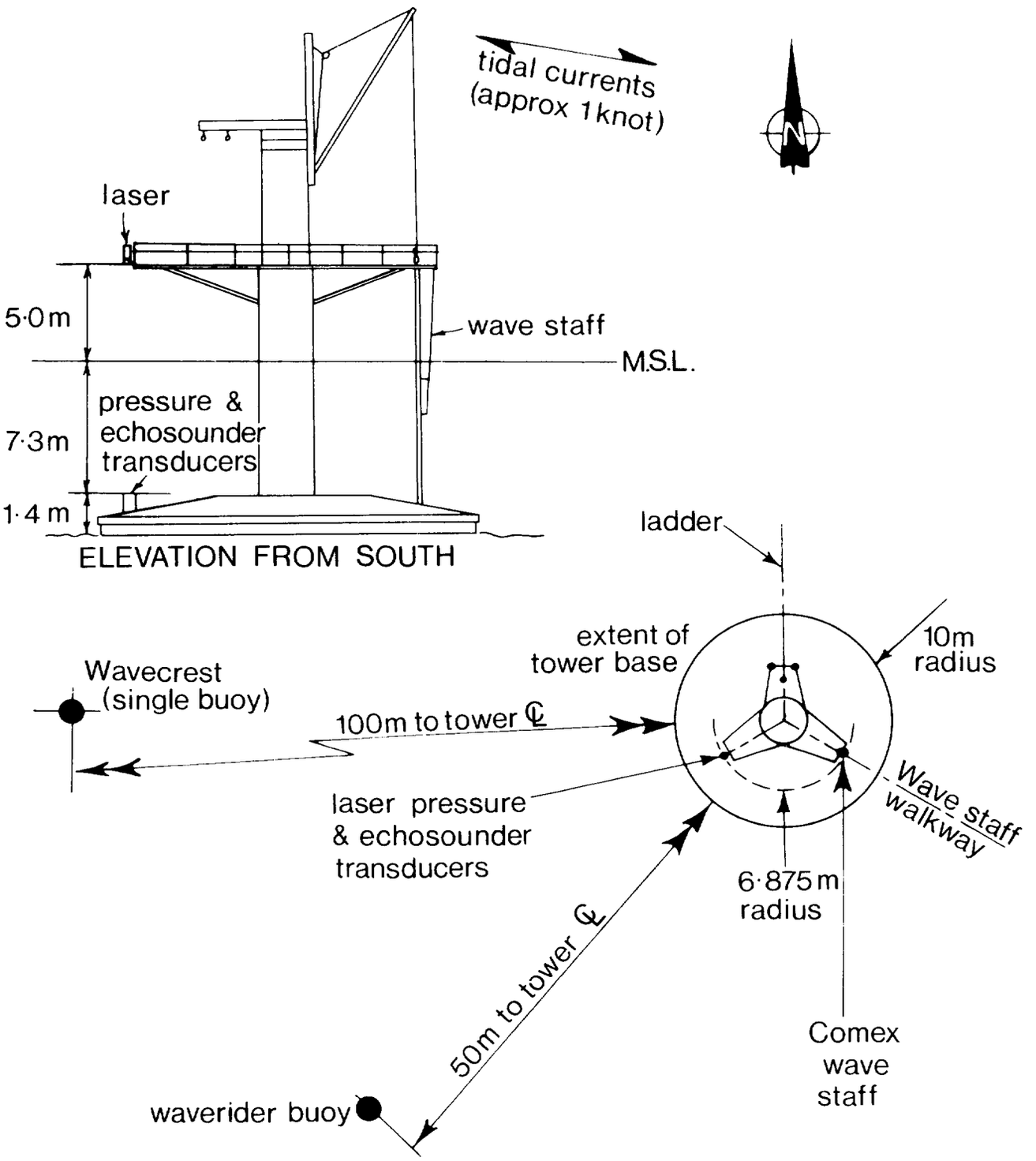

Fig. 1 Positions of wave measuring instruments.

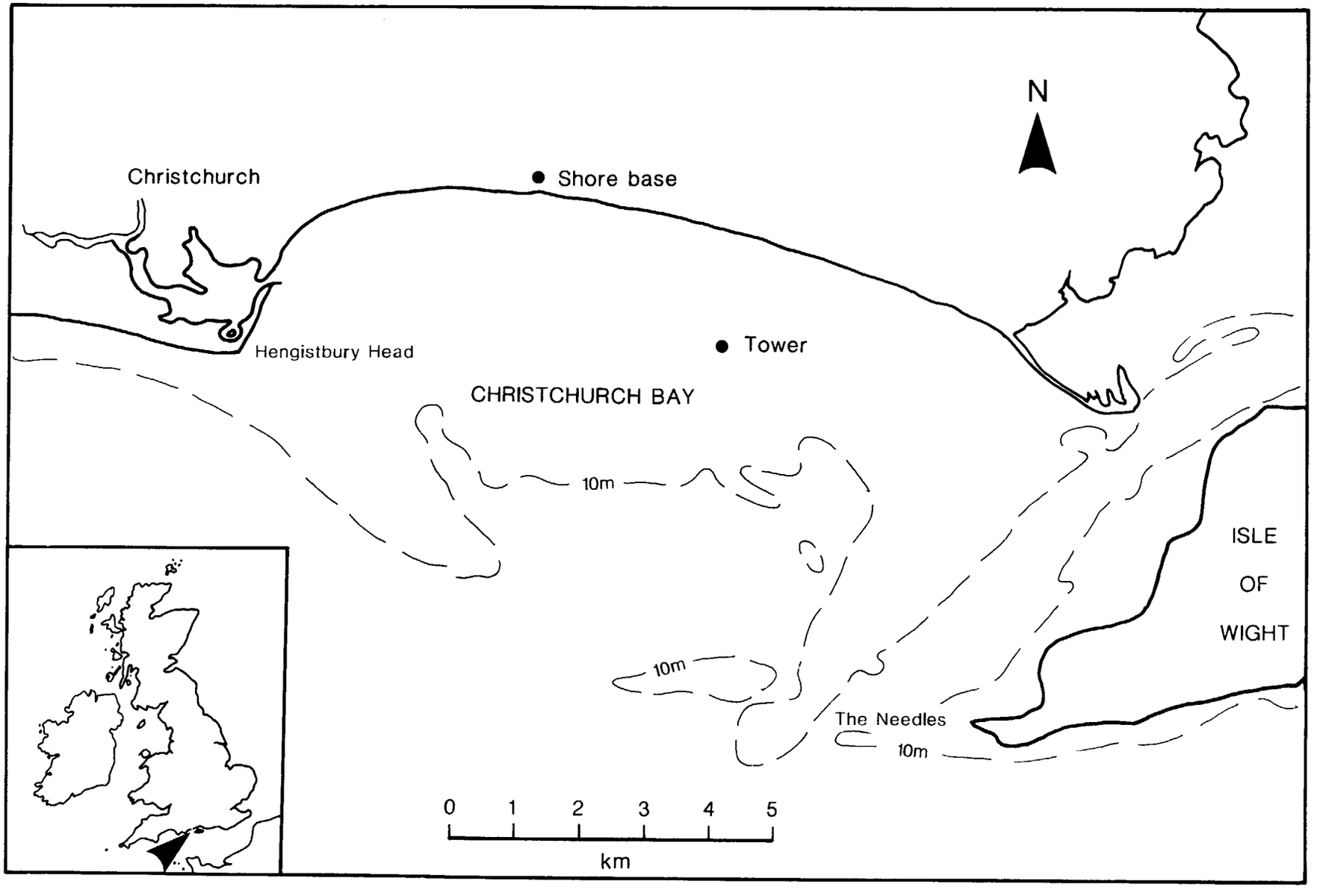

Fig. 2 Locations of tower and shore base.

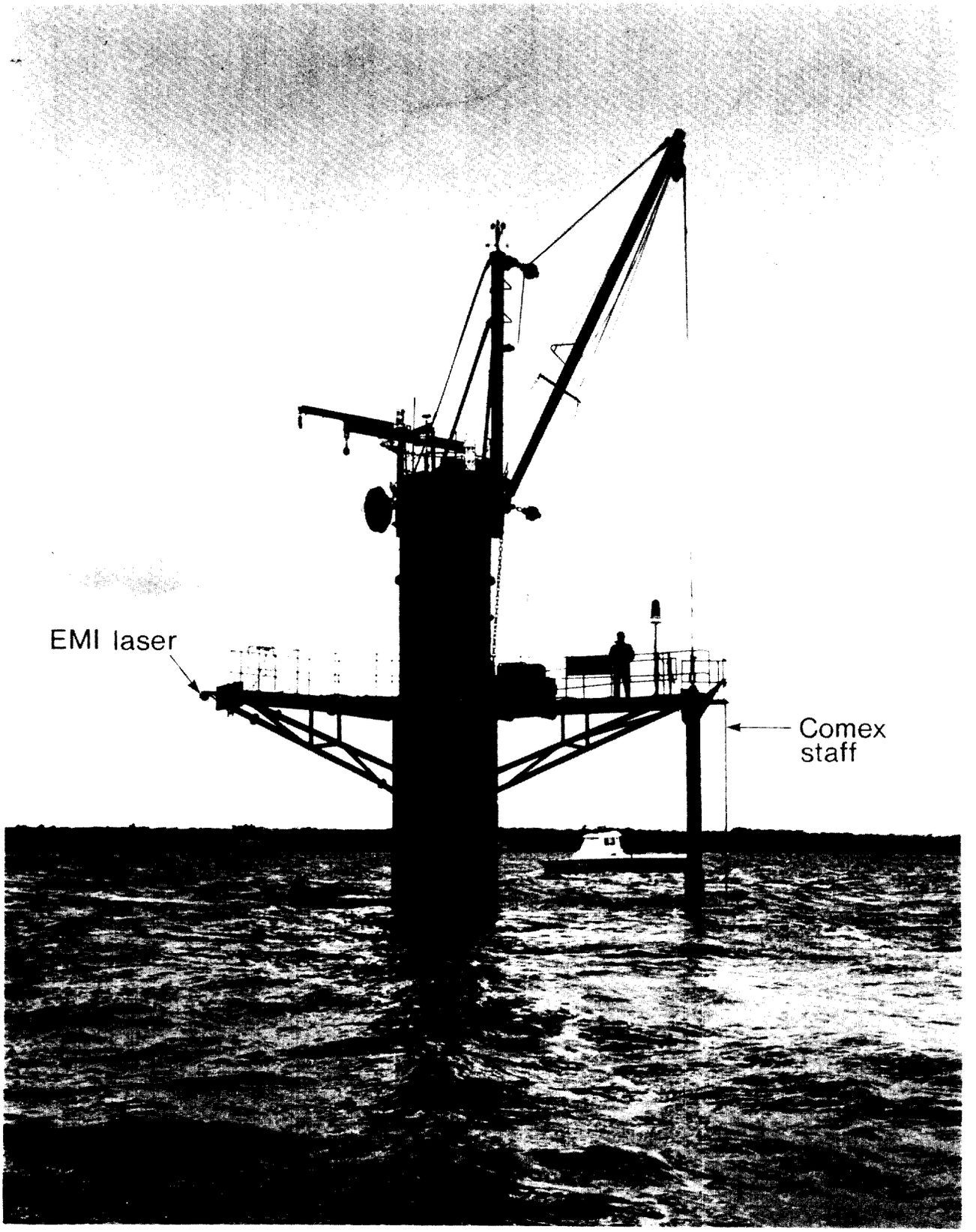

Fig. 3 Southerly aspect of tower.

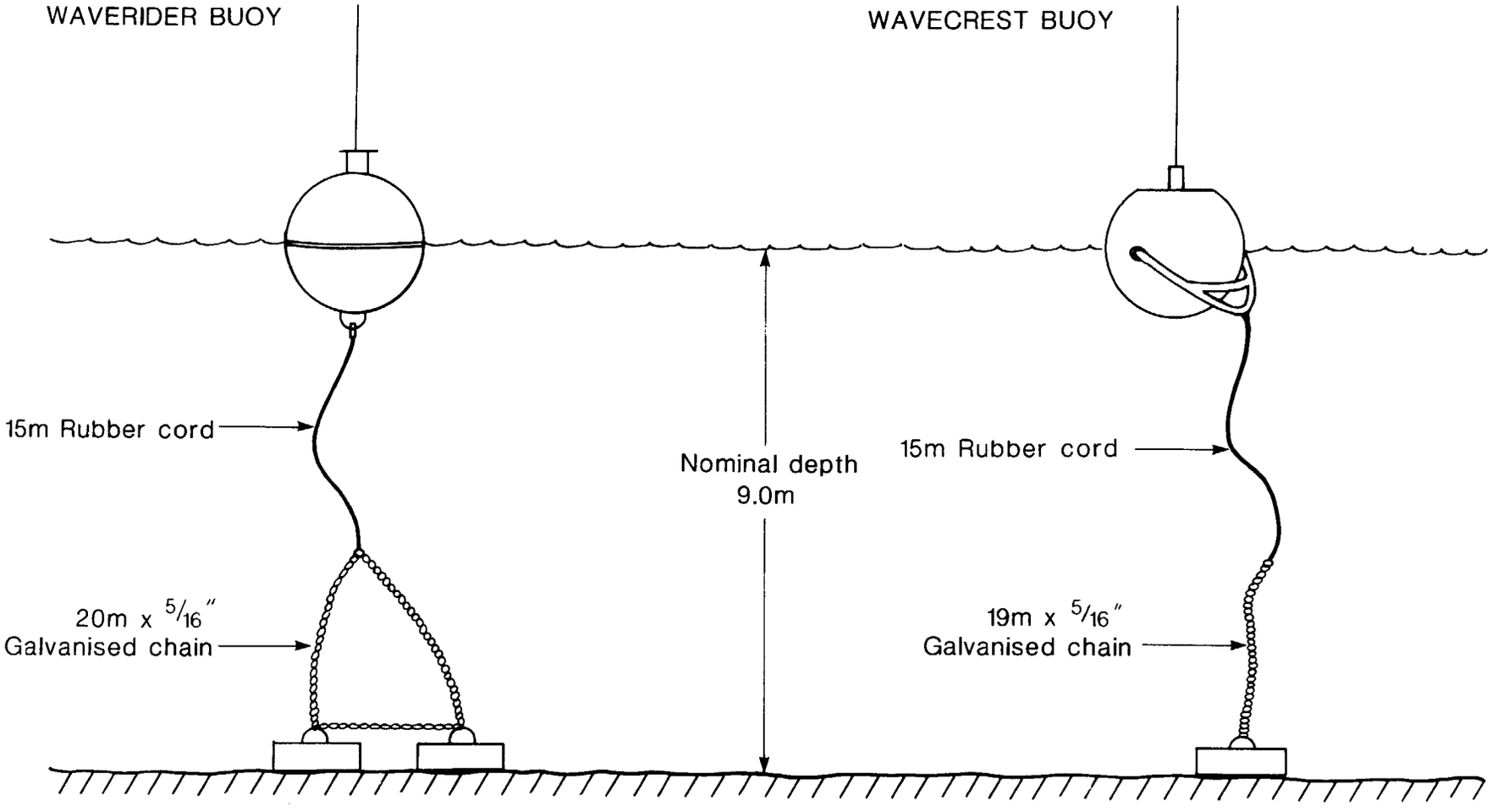

Fig. 4 Mooring configurations.

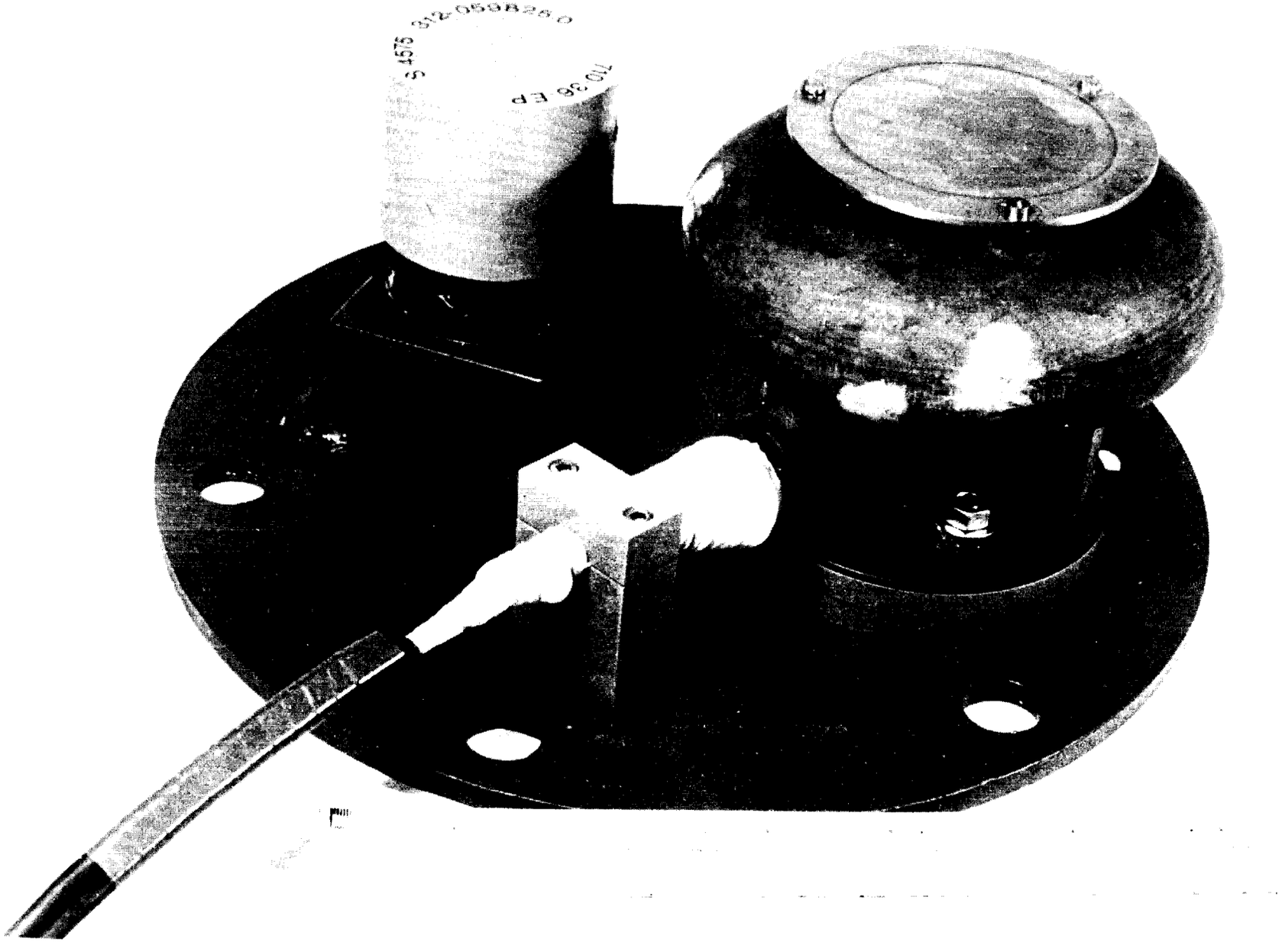

Fig. 5 Mounting arrangement for echo sounder and pressure sensor.

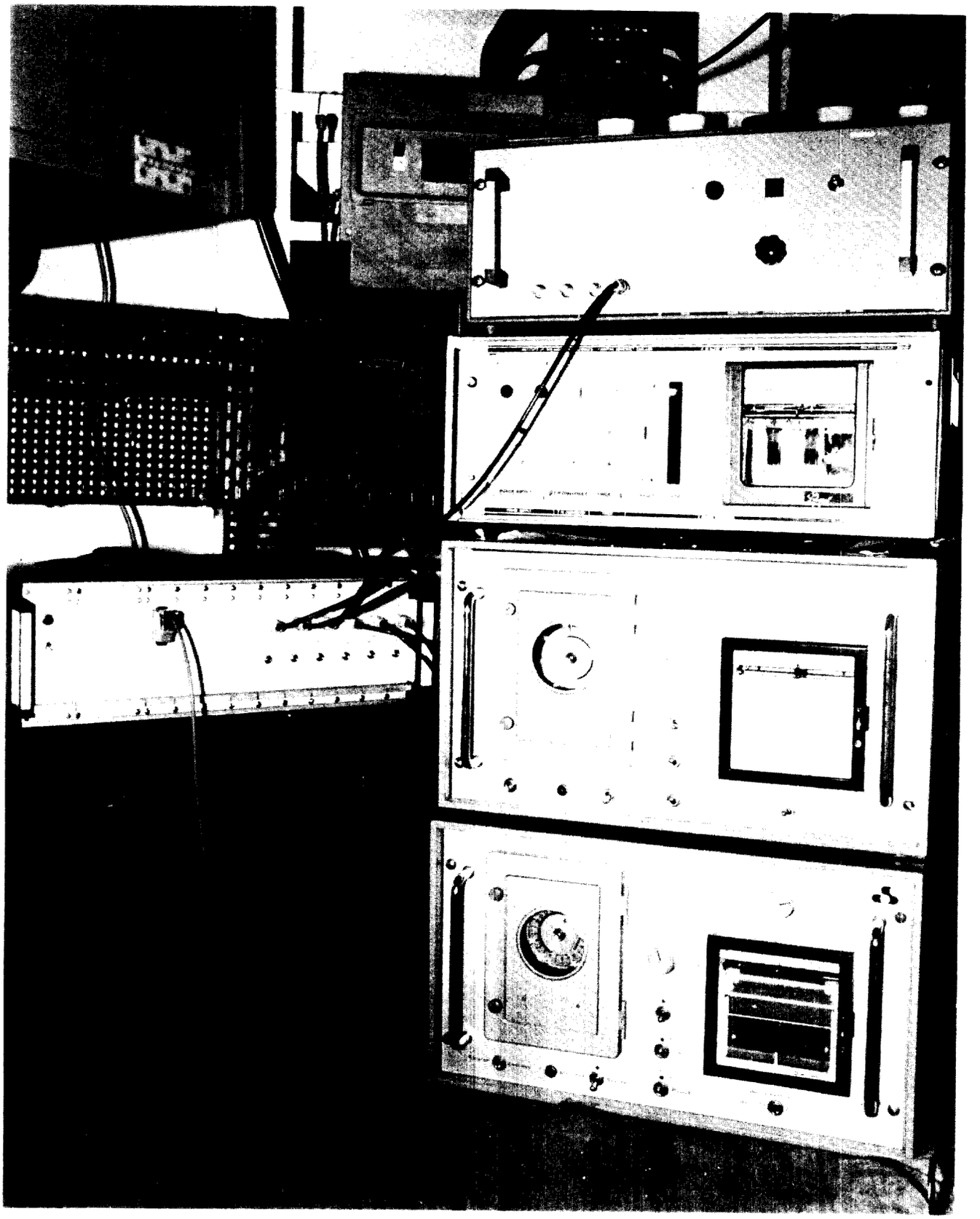

Fig. 6 Equipment arrangement in tower.

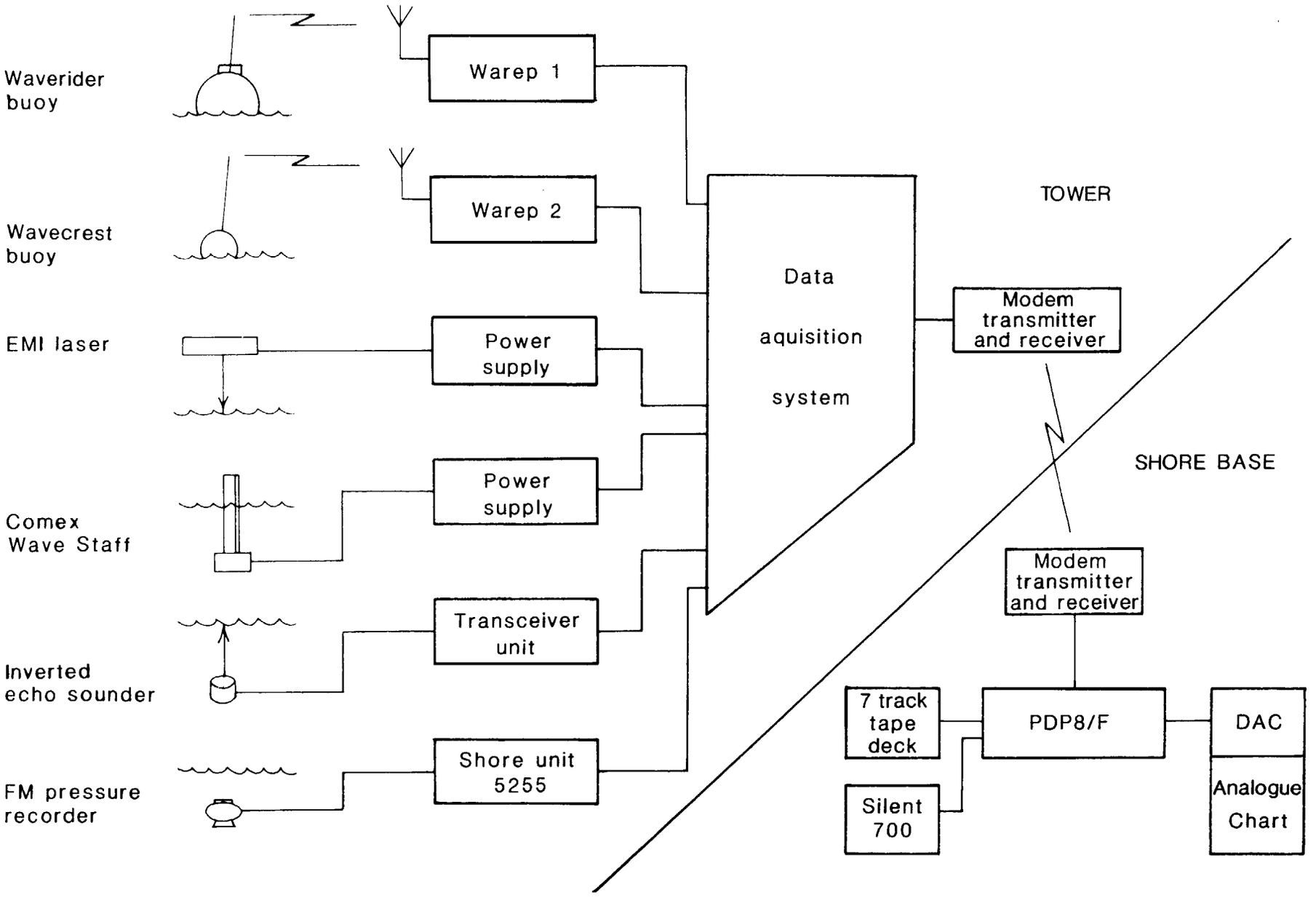

Fig. 7 System block diagram.

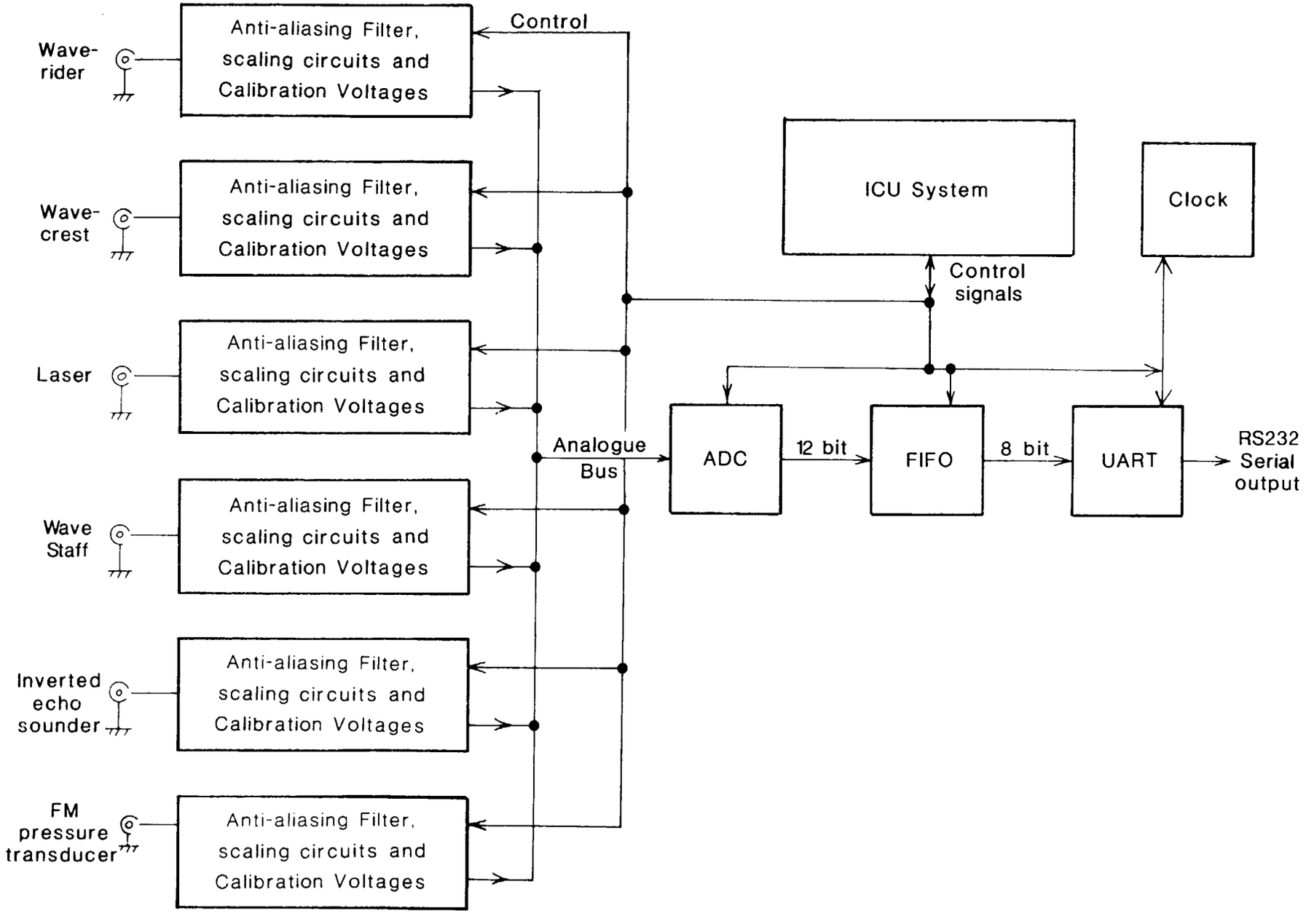

Fig. 8 Data acquisition schematic.

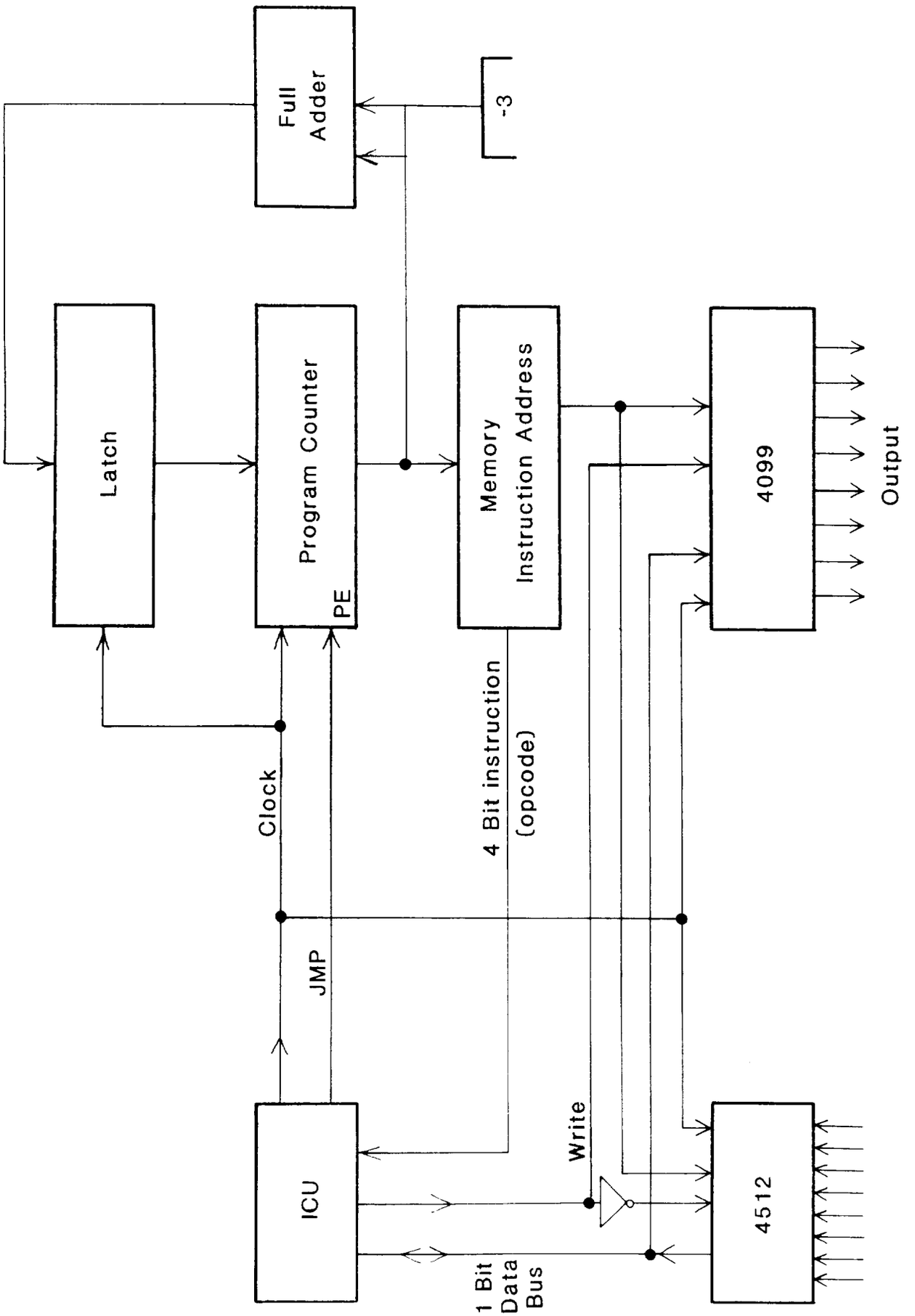

Fig. 9 ICU system.

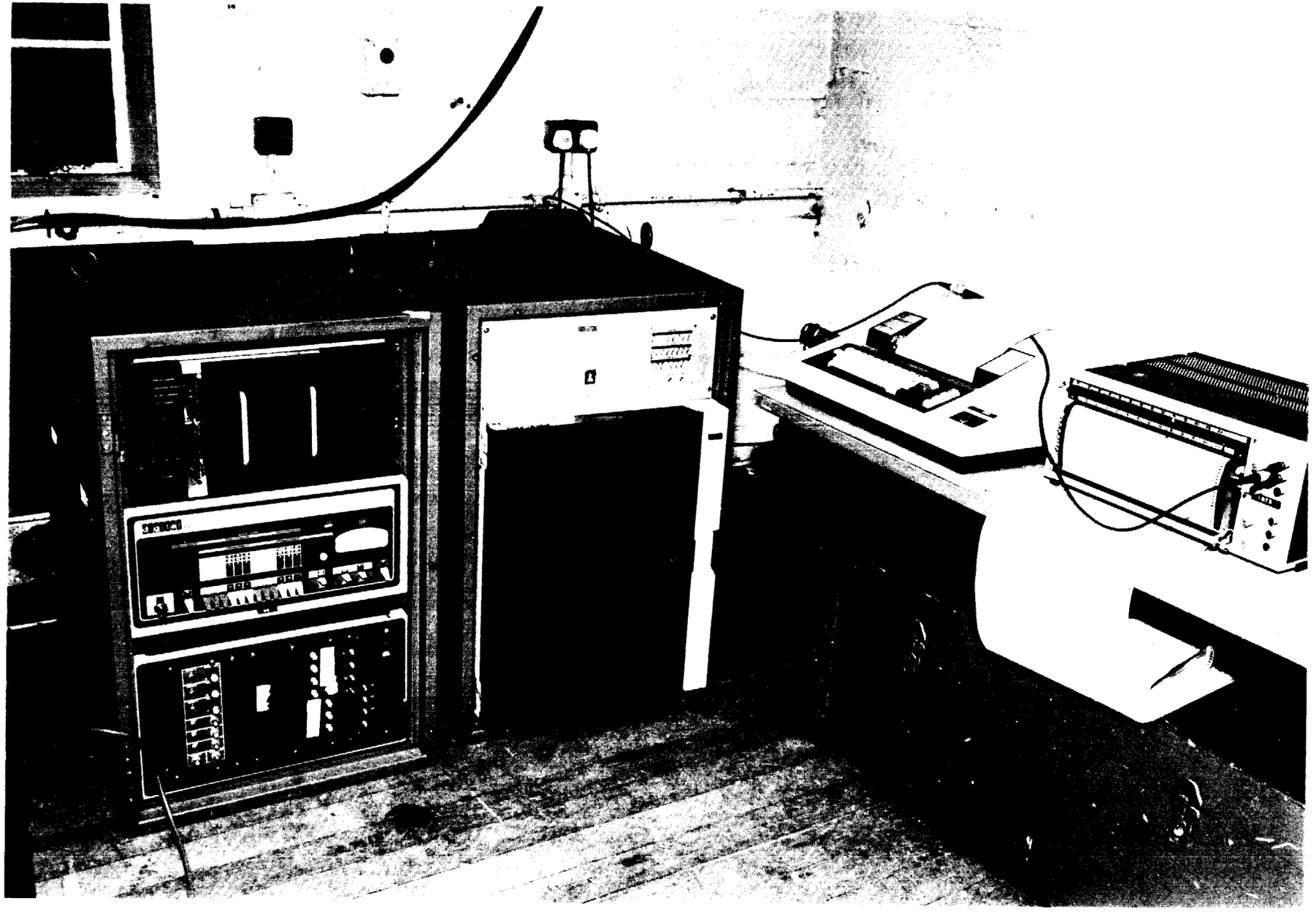

Fig. 10 Equipment arrangement at shore base.

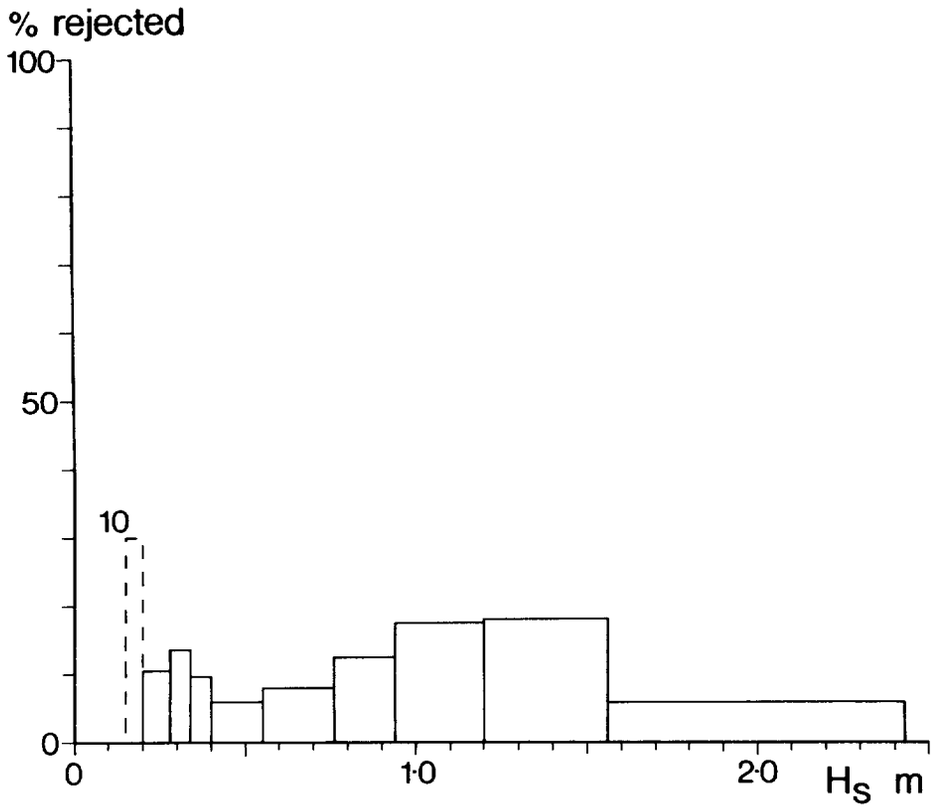

Figure 11a EMI laser. Percentage of rejected records by classes of significant wave height.

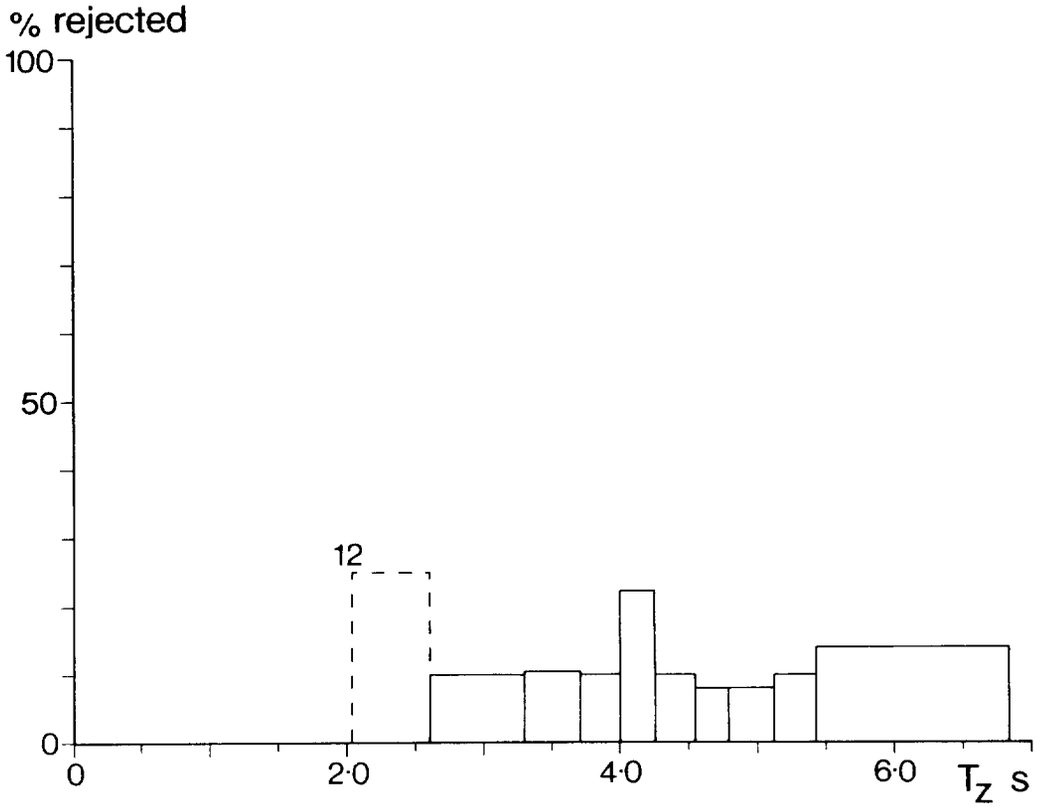

Figure 11b EMI laser. Percentage of rejected records by classes of zero crossing period.

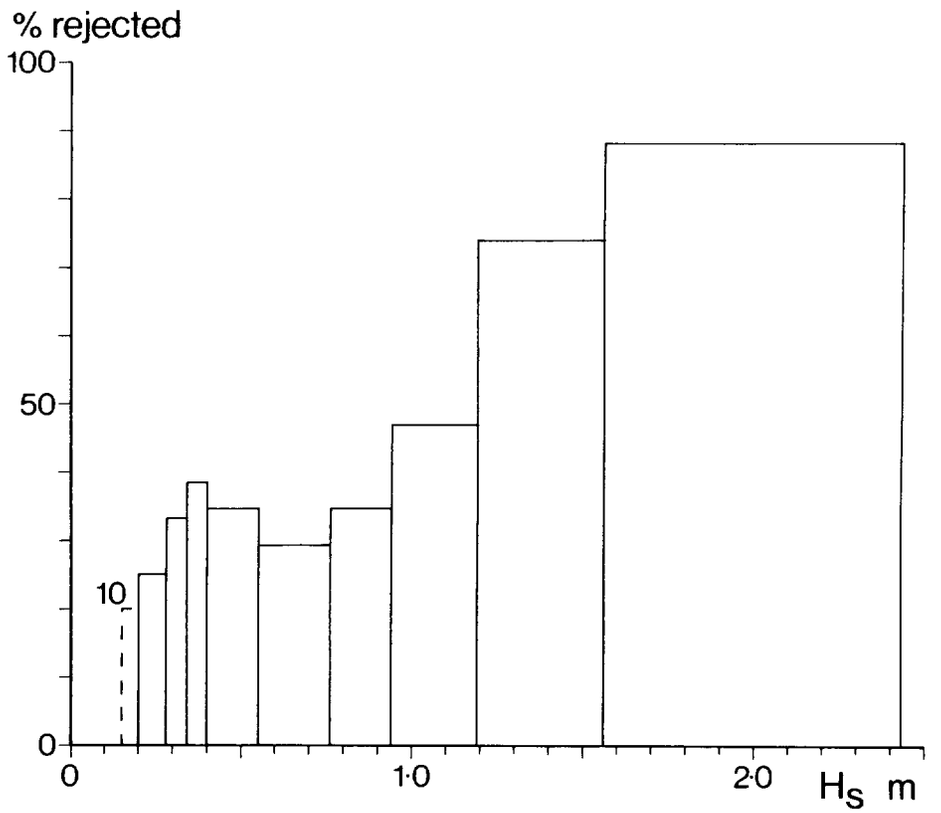

Figure 12a SIMRAD echo sounder. Percentage of rejected records by classes of significant wave height.

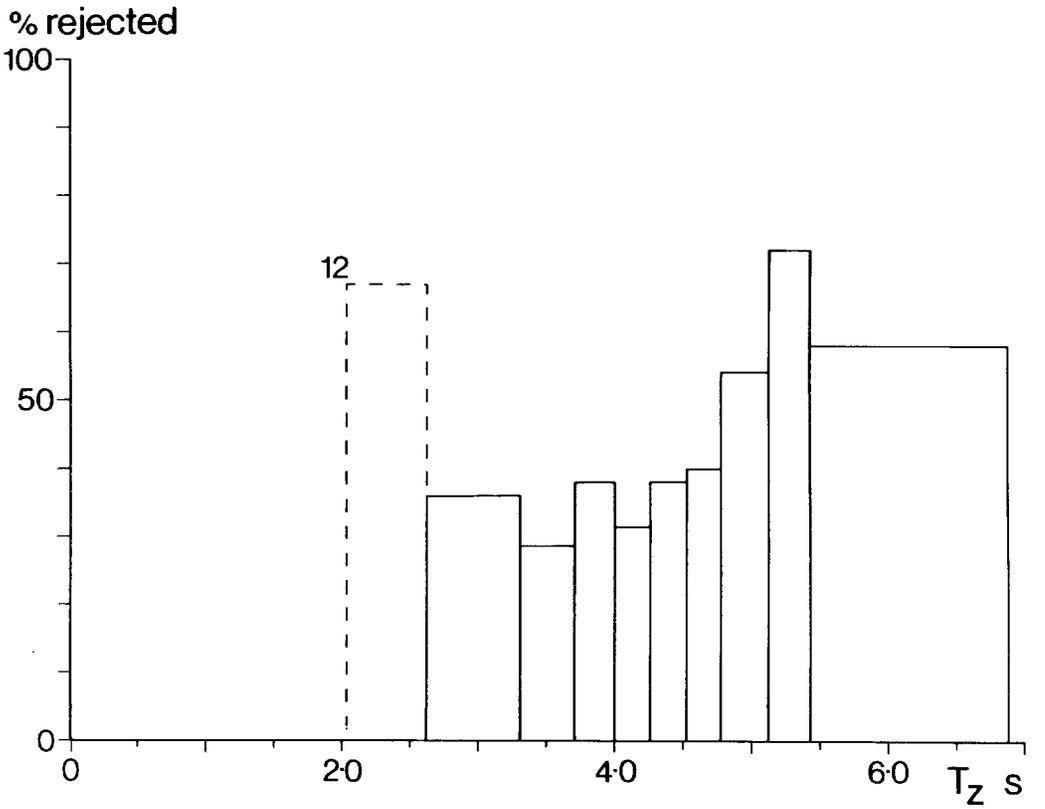

Figure 12b SIMRAD echo sounder. Percentage of rejected records by classes of zero crossing period.

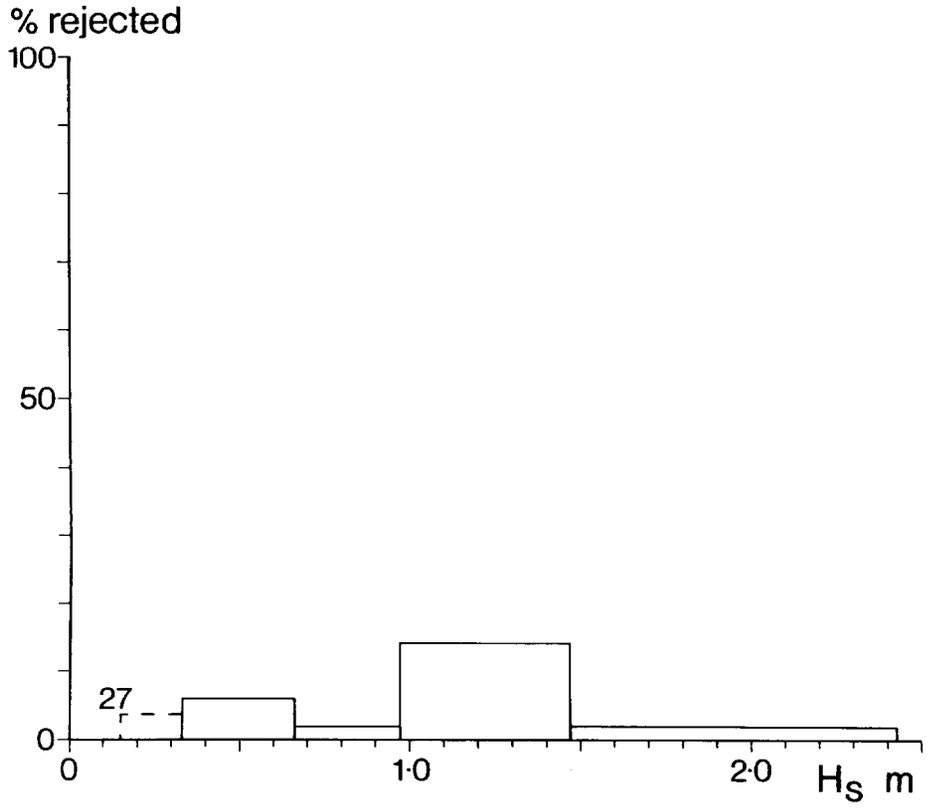

Figure 13a COMEX wave staff. Percentage of rejected records by classes of significant wave height.

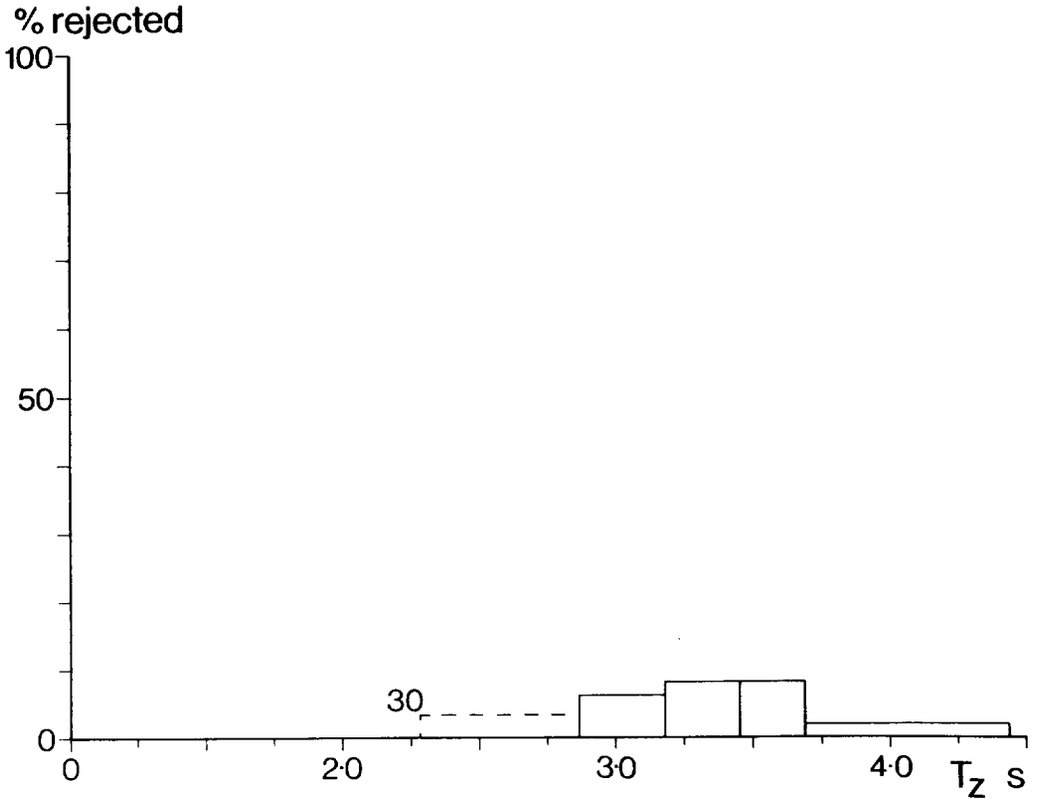

Figure 13b COMEX wave staff. Percentage of rejected records by classes of zero crossing period.

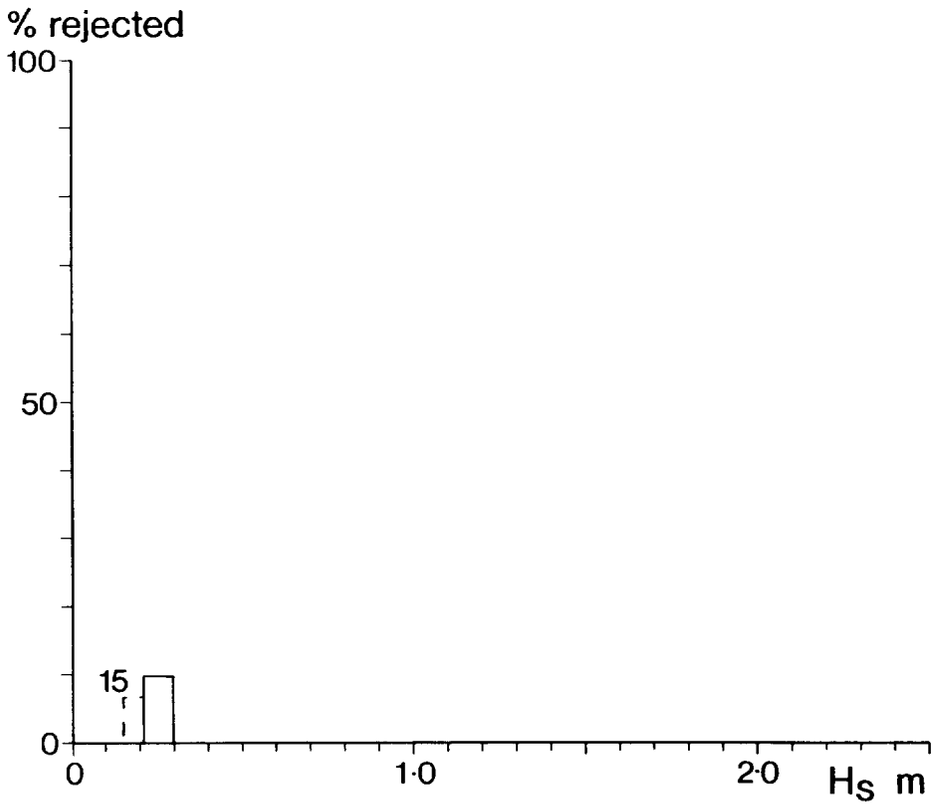

Figure 14a FM pressure recorder. Percentage of rejected records by classes of significant wave height.

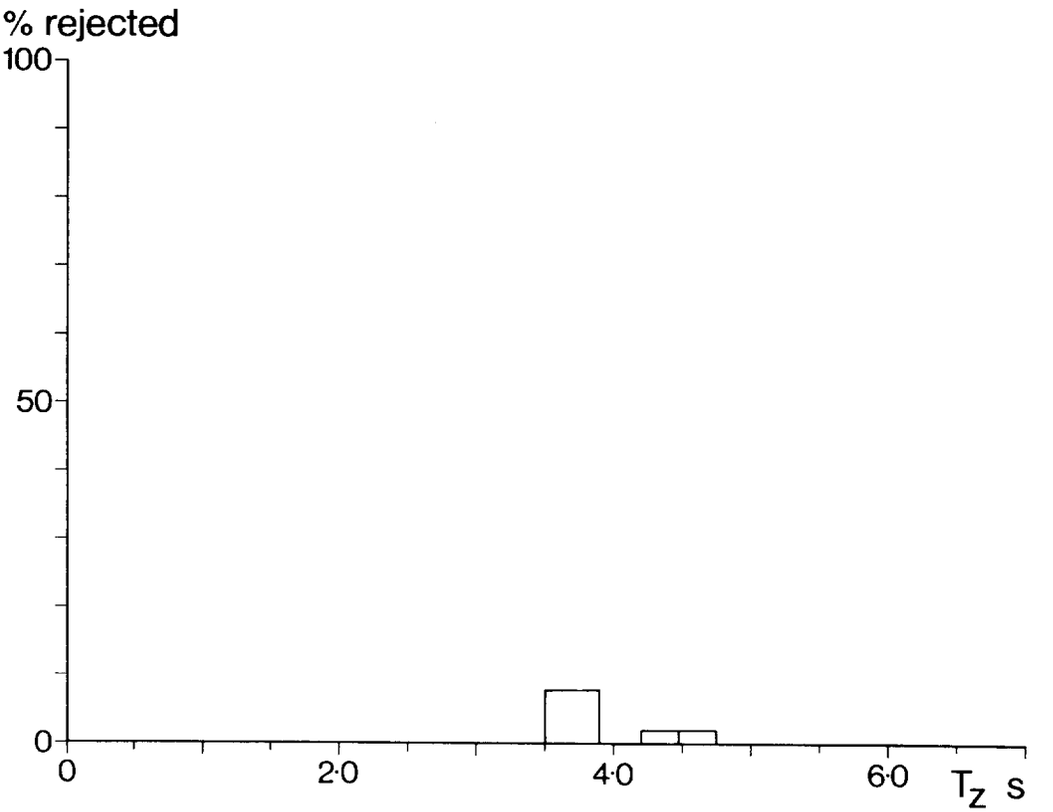

Figure 14b FM pressure recorder. Percentage of rejected records by classes of zero crossing period.

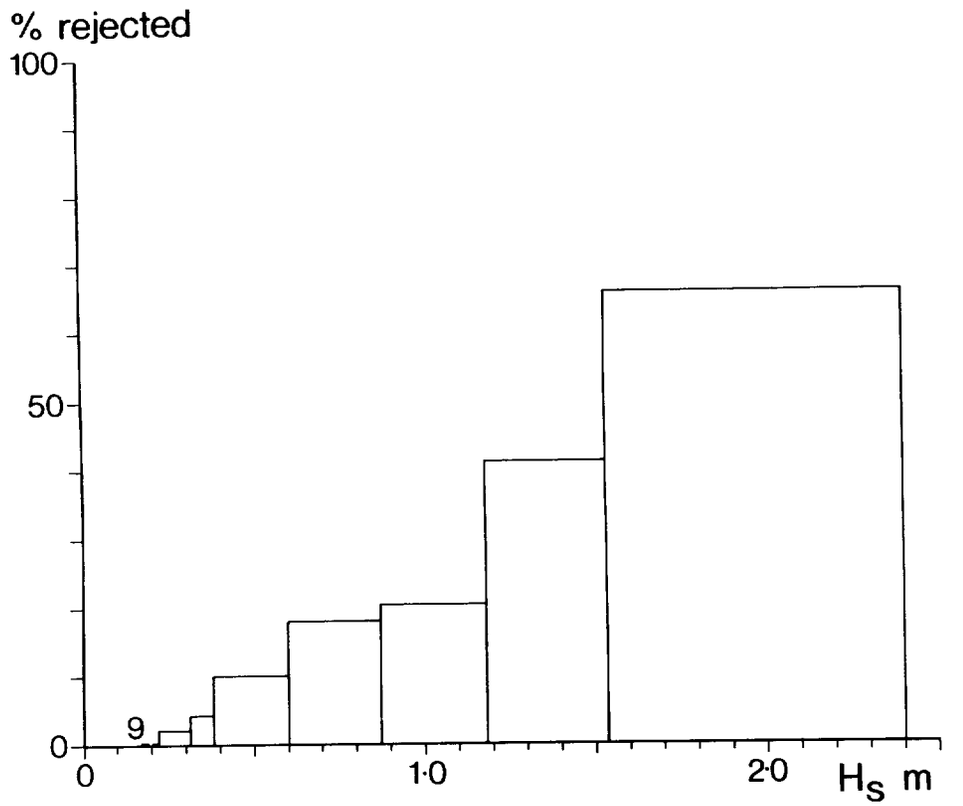

Figure 15a NBA Wavecrest. Percentage of rejected records by classes of significant wave height.

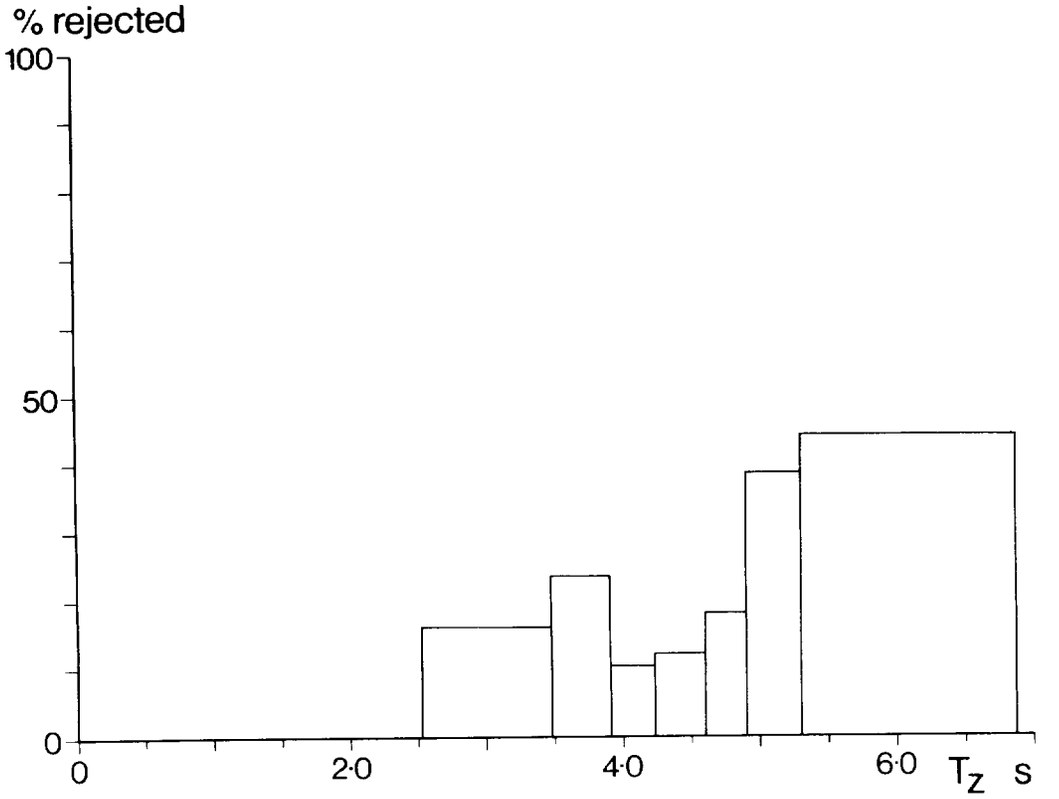

Figure 15b NBA Wavecrest. Percentage of rejected records by classes of zero crossing period.

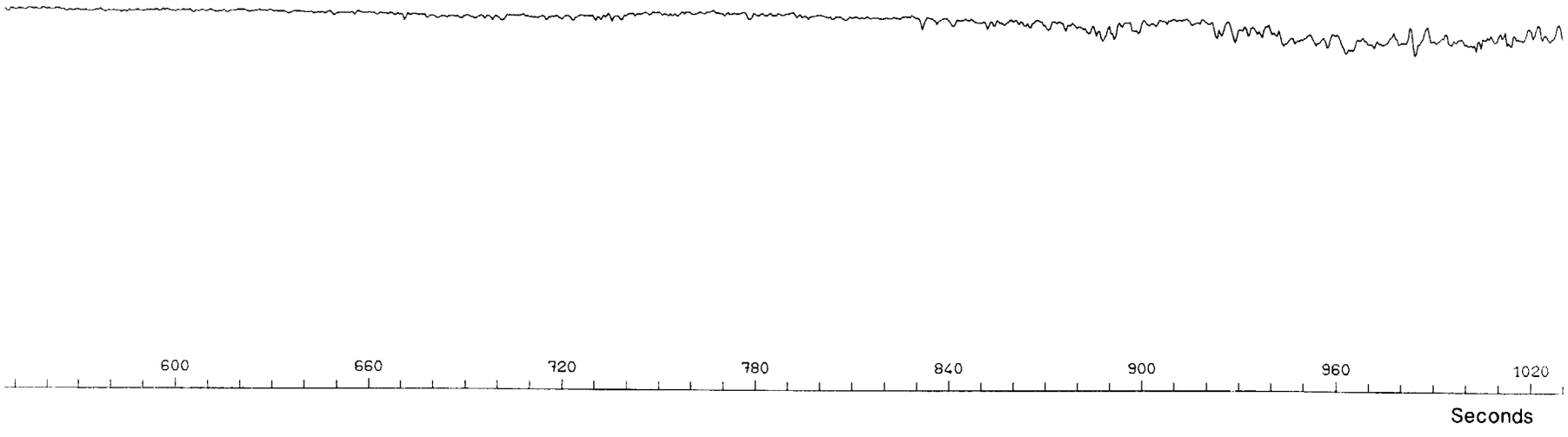

Figure 16 Example of faulty trace returned by EMI laser under foggy conditions

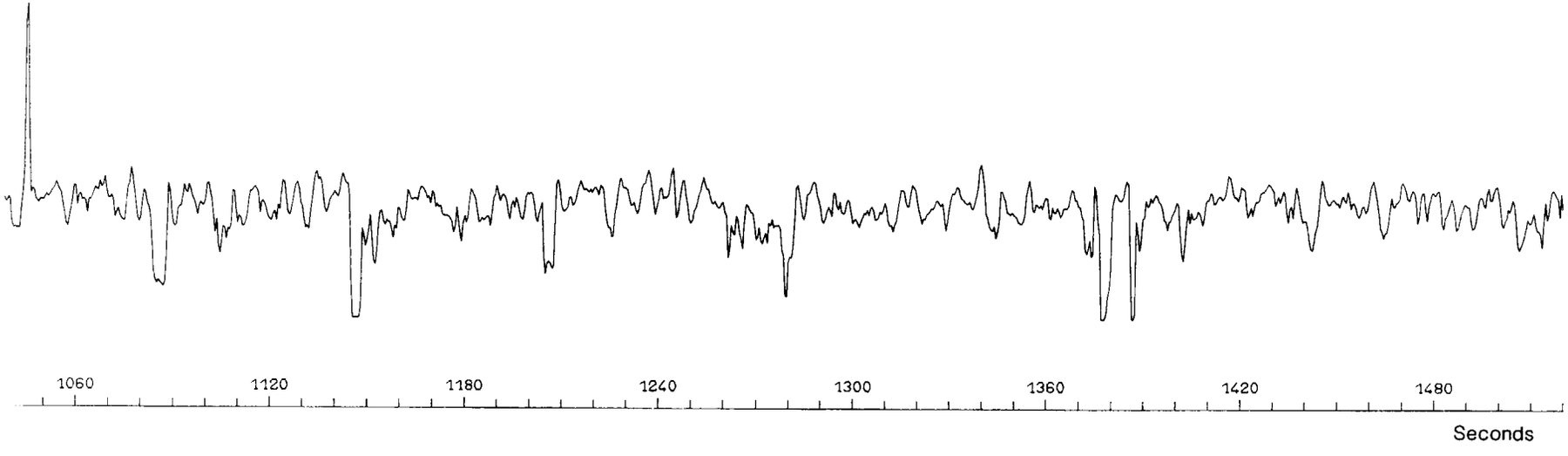

Figure 17 Example of faulty trace returned by SIMRAD echo sounder.

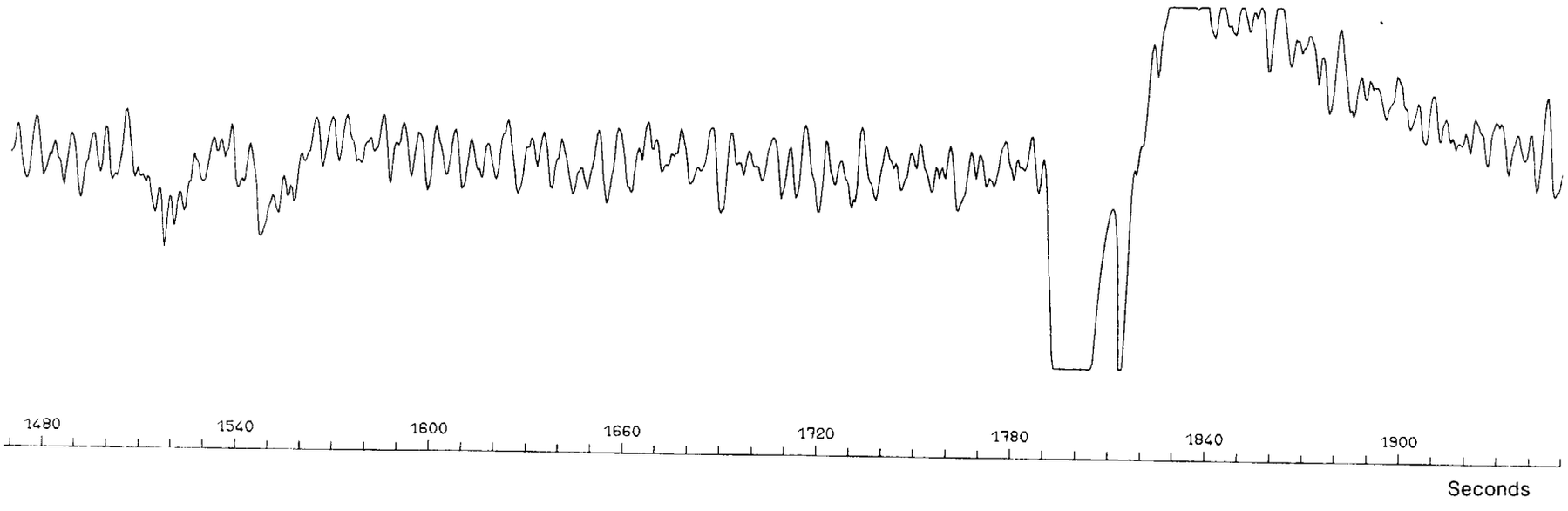

Figure 18 Example of faulty trace returned by NBA Wavecrest.

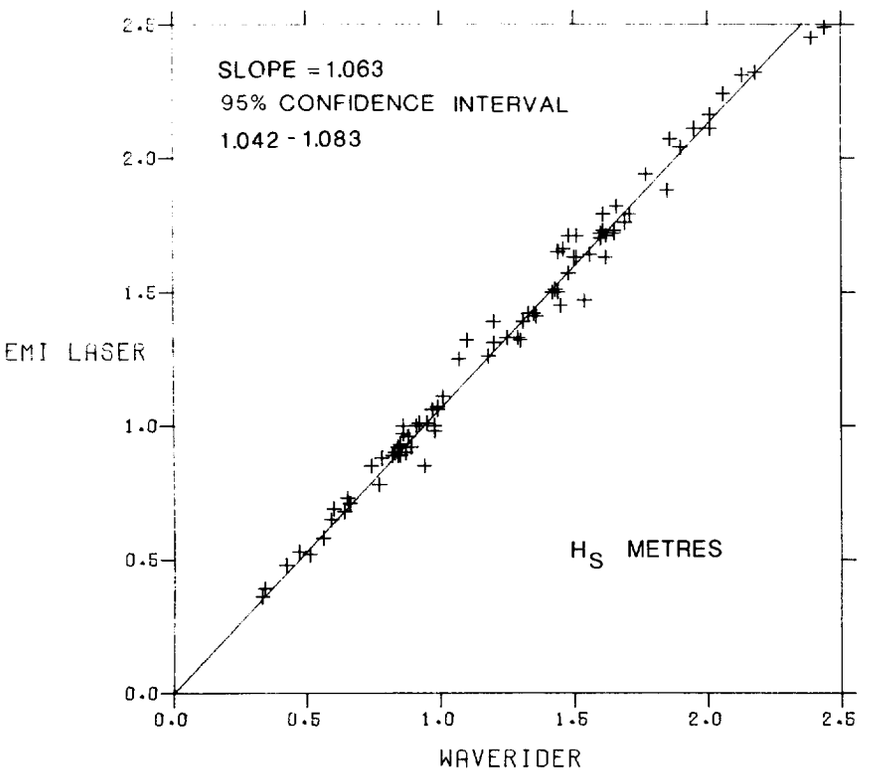

Figure 19a EMI laser .v. Datawell Waverider. Comparison of significant wave height.

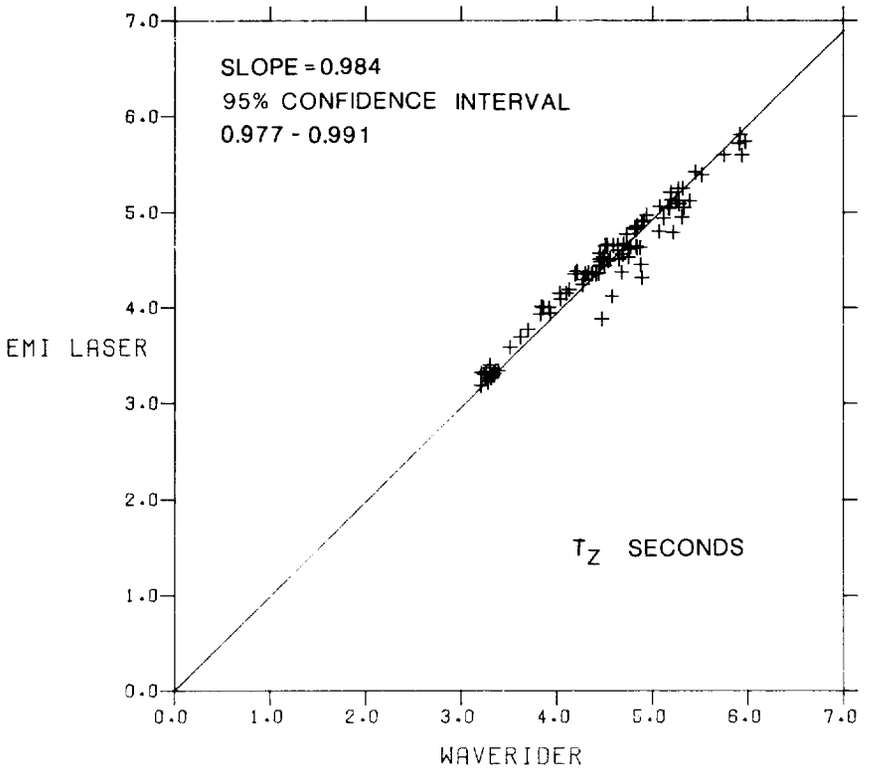

Figure 19b EMI laser .v. Datawell Waverider. Comparison of mean zero crossing period.

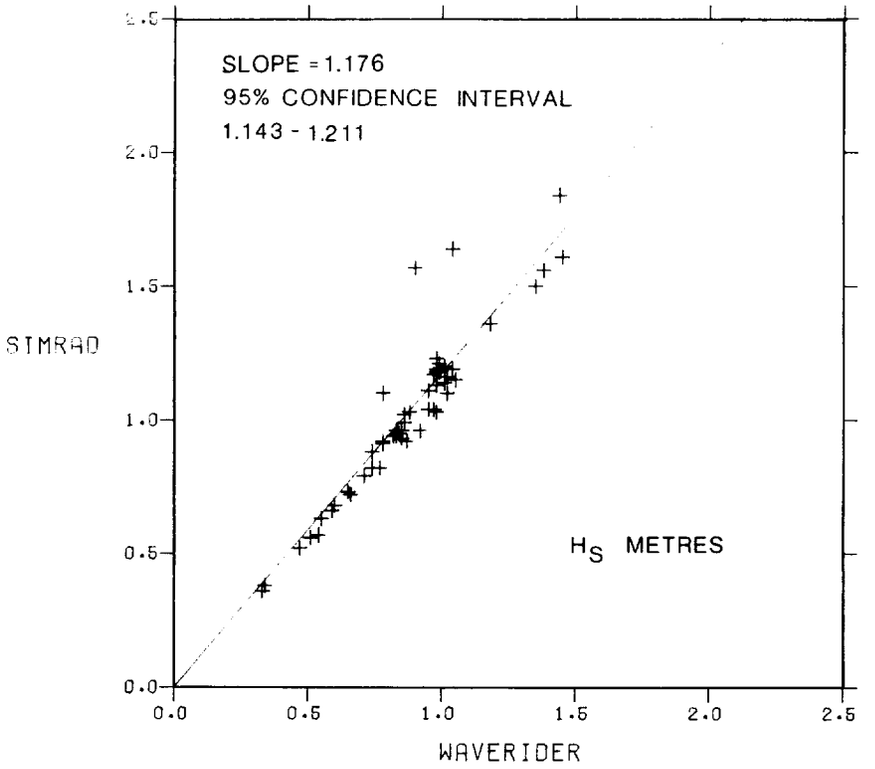

Figure 20a SIMRAD echo sounder .v. Datawell Waverider. Comparison of significant wave height.

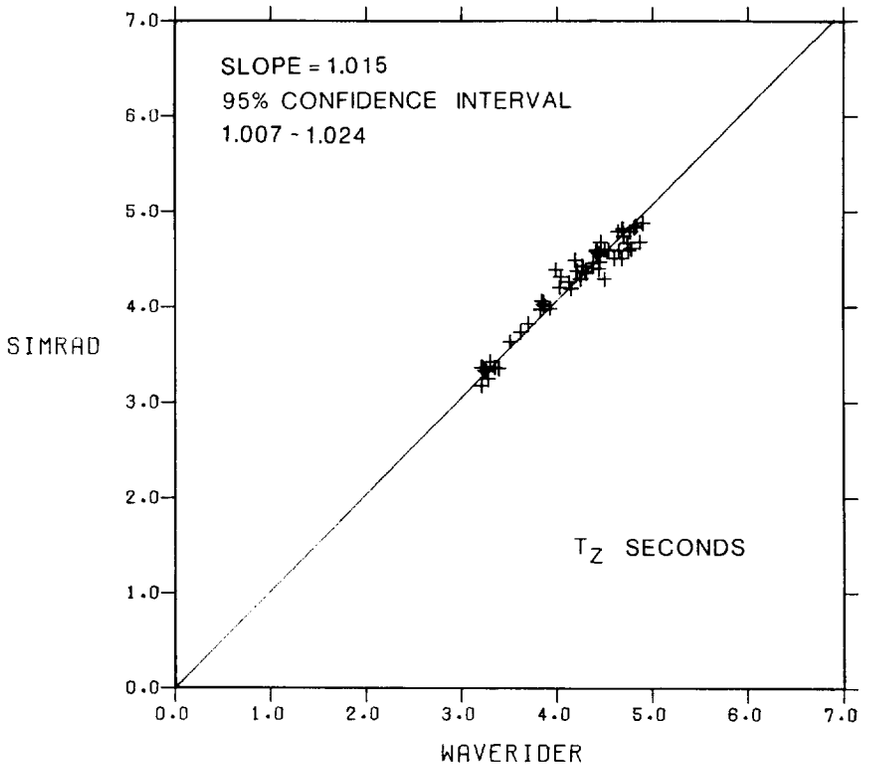

Figure 20b SIMRAD echo sounder .v. Datawell Waverider. Comparison of mean zero crossing period.

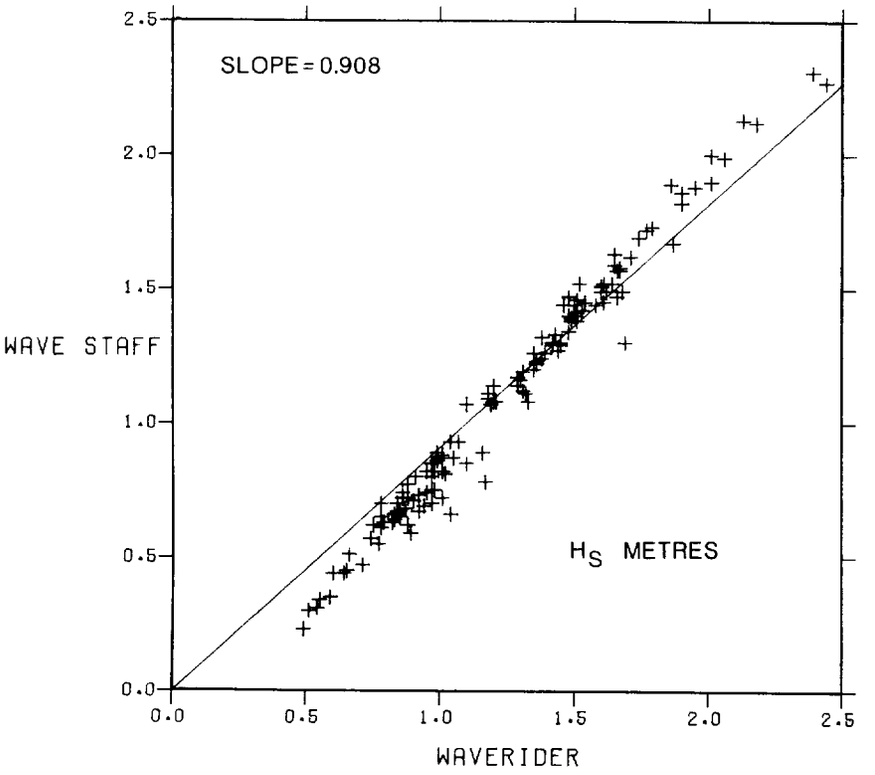

Figure 21a COMEX wave staff .v. Datawell Waverider. Comparison of significant wave height.

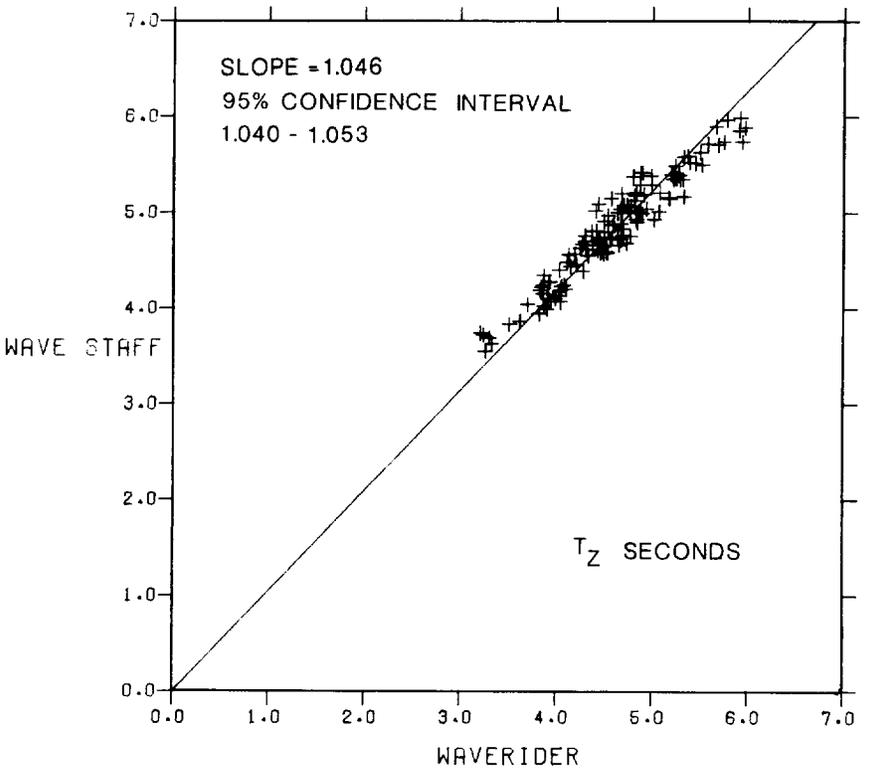

Figure 21b COMEX wave staff .v. Datawell Waverider. Comparison of mean zero crossing period.

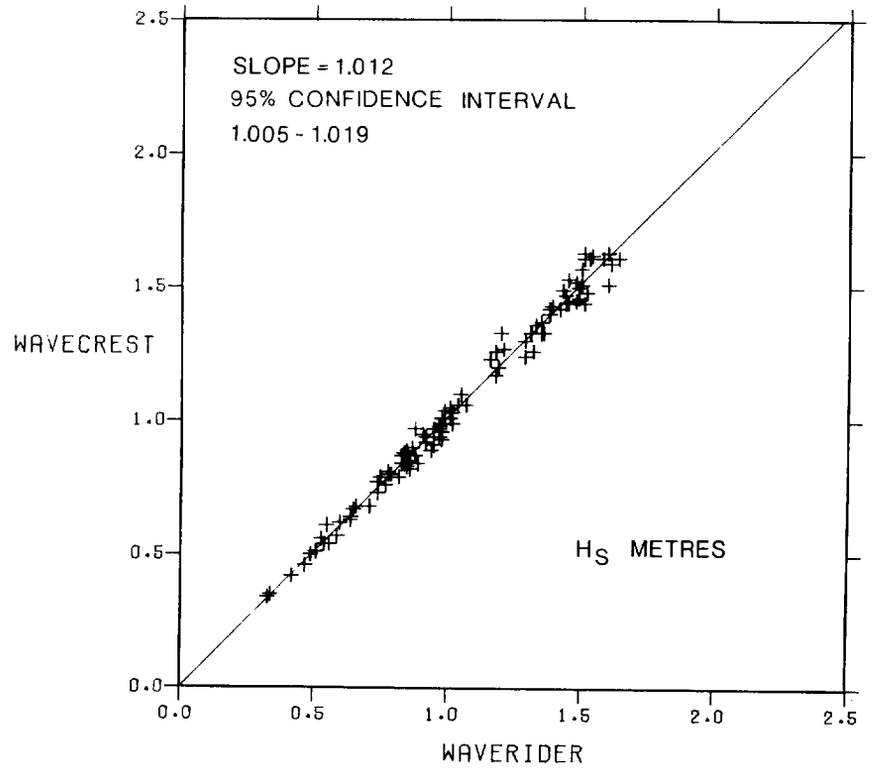

Figure 22a NBA Wavecrest .v. Datawell Waverider. Comparison of significant wave height.

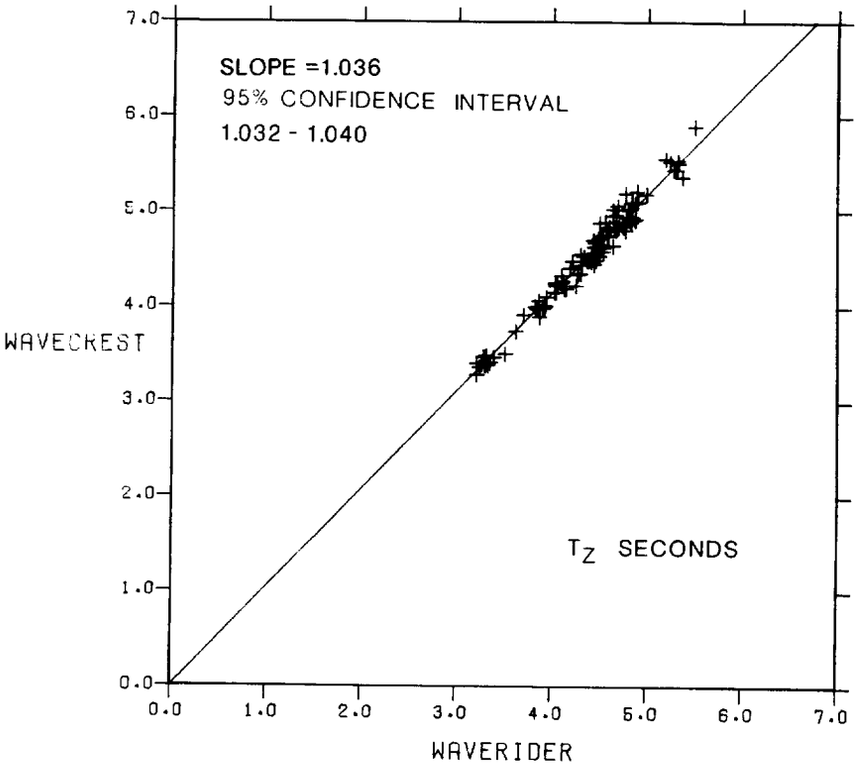

Figure 22b NBA Wavecrest .v. Datawell Waverider. Comparison of mean zero crossing period.

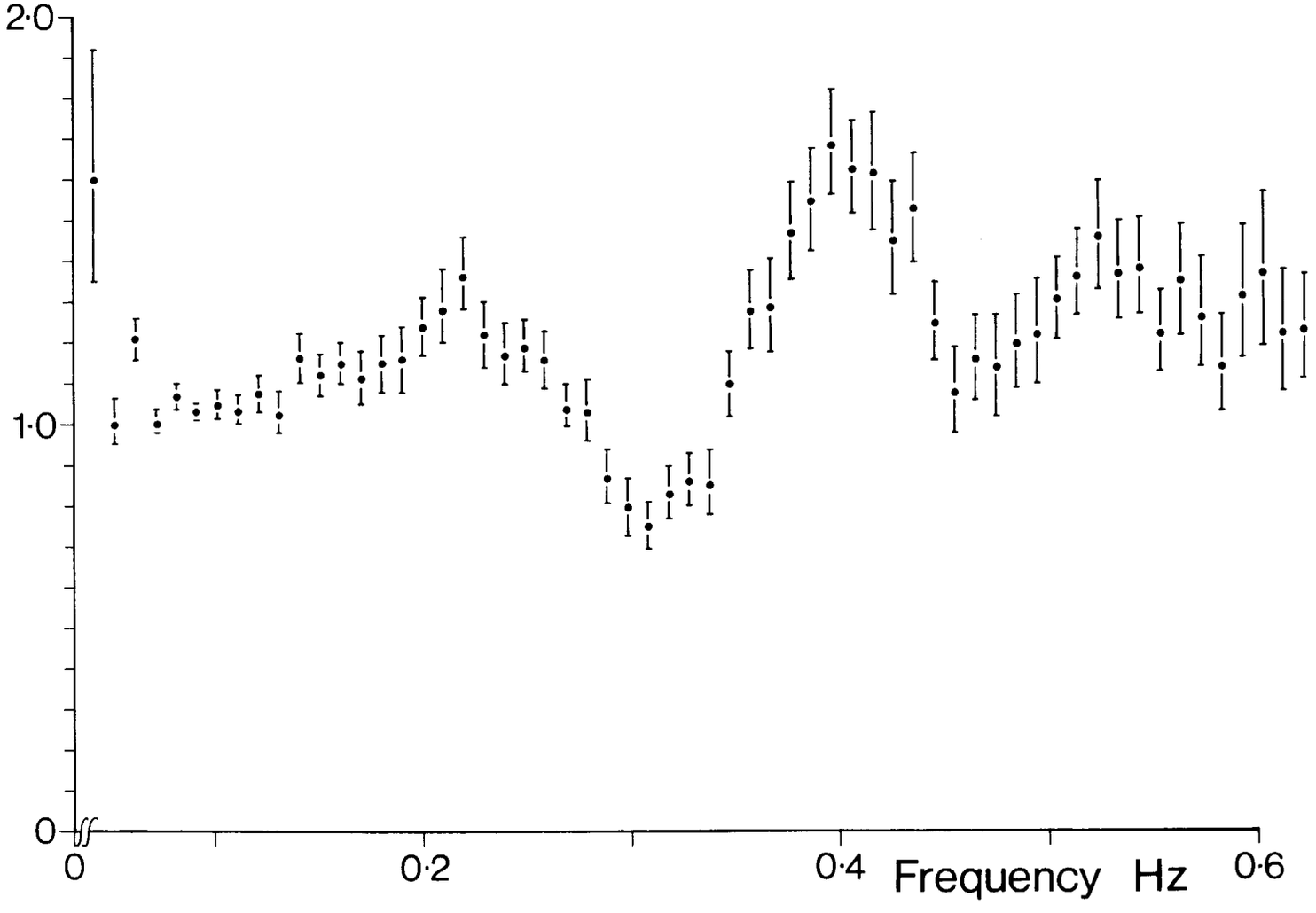

Figure 23 EMI laser .v. Datawell Waverider. Slope, • , and 95% confidence interval on slope, I , of reduced major axis regression line (constrained through 0,0) fitted to the population of simultaneous spectral densities at each frequency.

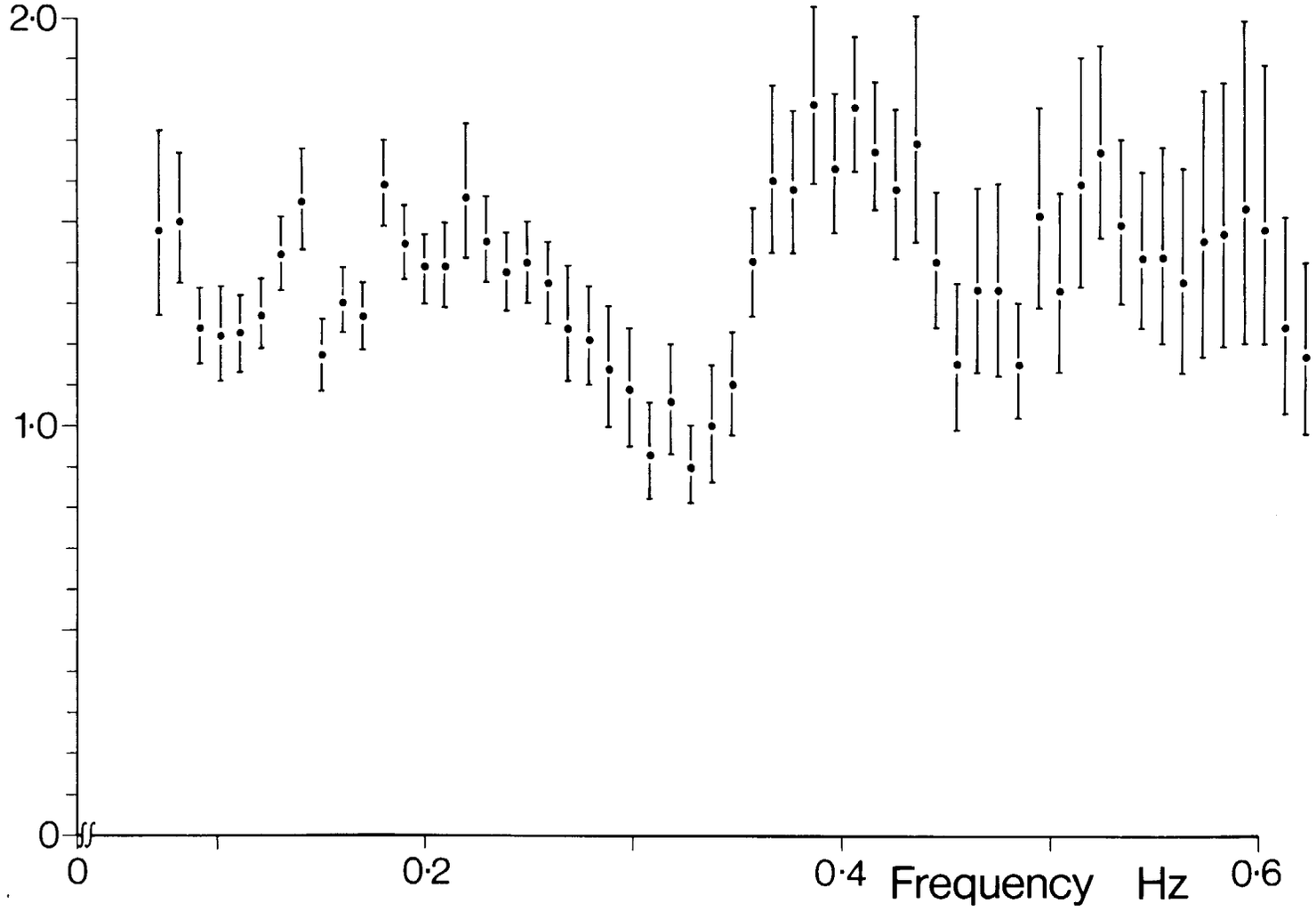

Figure 24 SIMRAD echo sounder .v. Datawell Waverider. Slope, • , and 95% confidence interval on slope, I , of reduced major axis regression line (constrained through 0,0) fitted to the population of simultaneous spectral densities at each frequency.

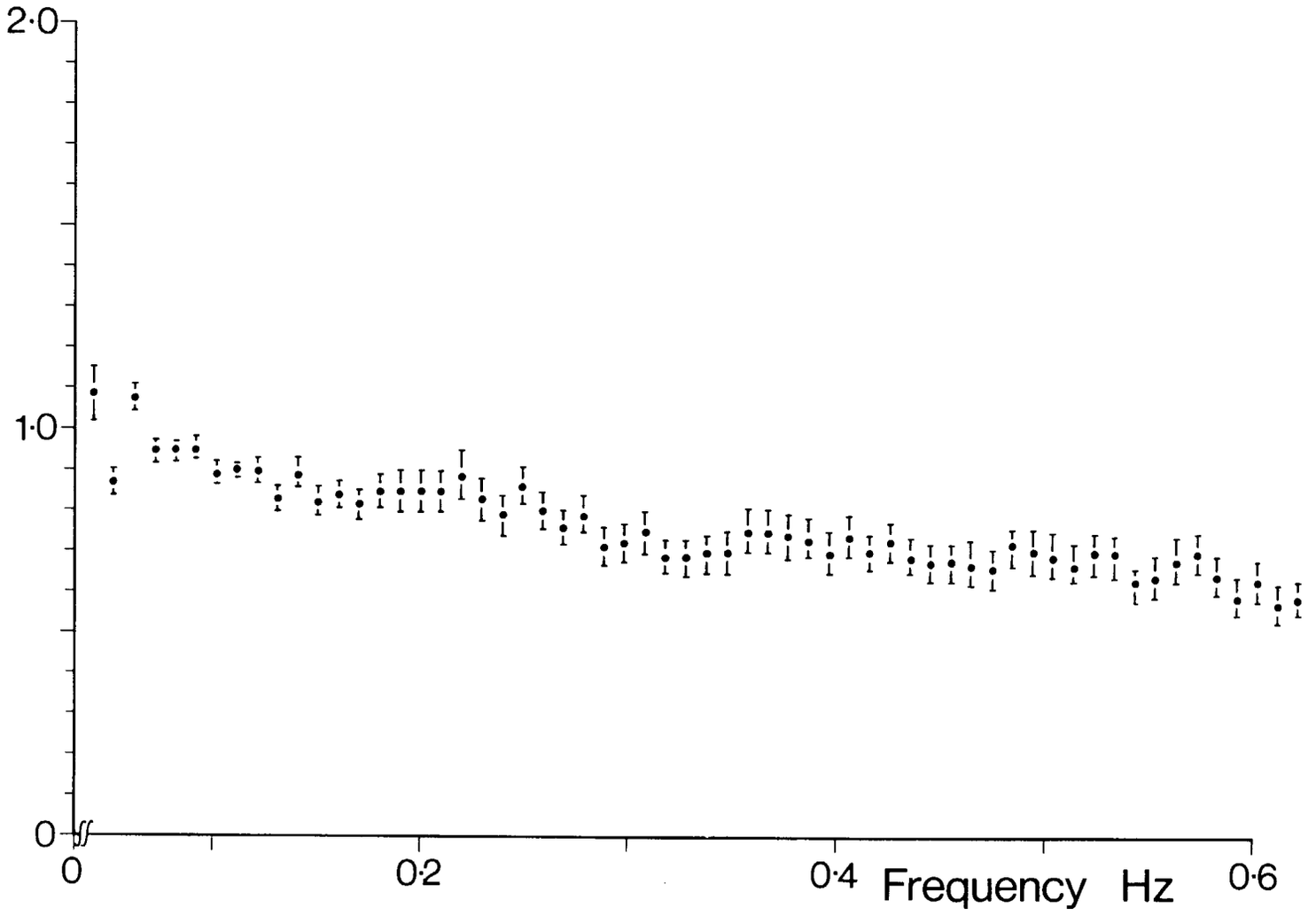

Figure 25 COMEX wave staff .v. Datawell Waverider. Slope, • , and 95% confidence interval on slope, I , of reduced major axis regression line (constrained through 0,0) fitted to the population of simultaneous spectral densities at each frequency.

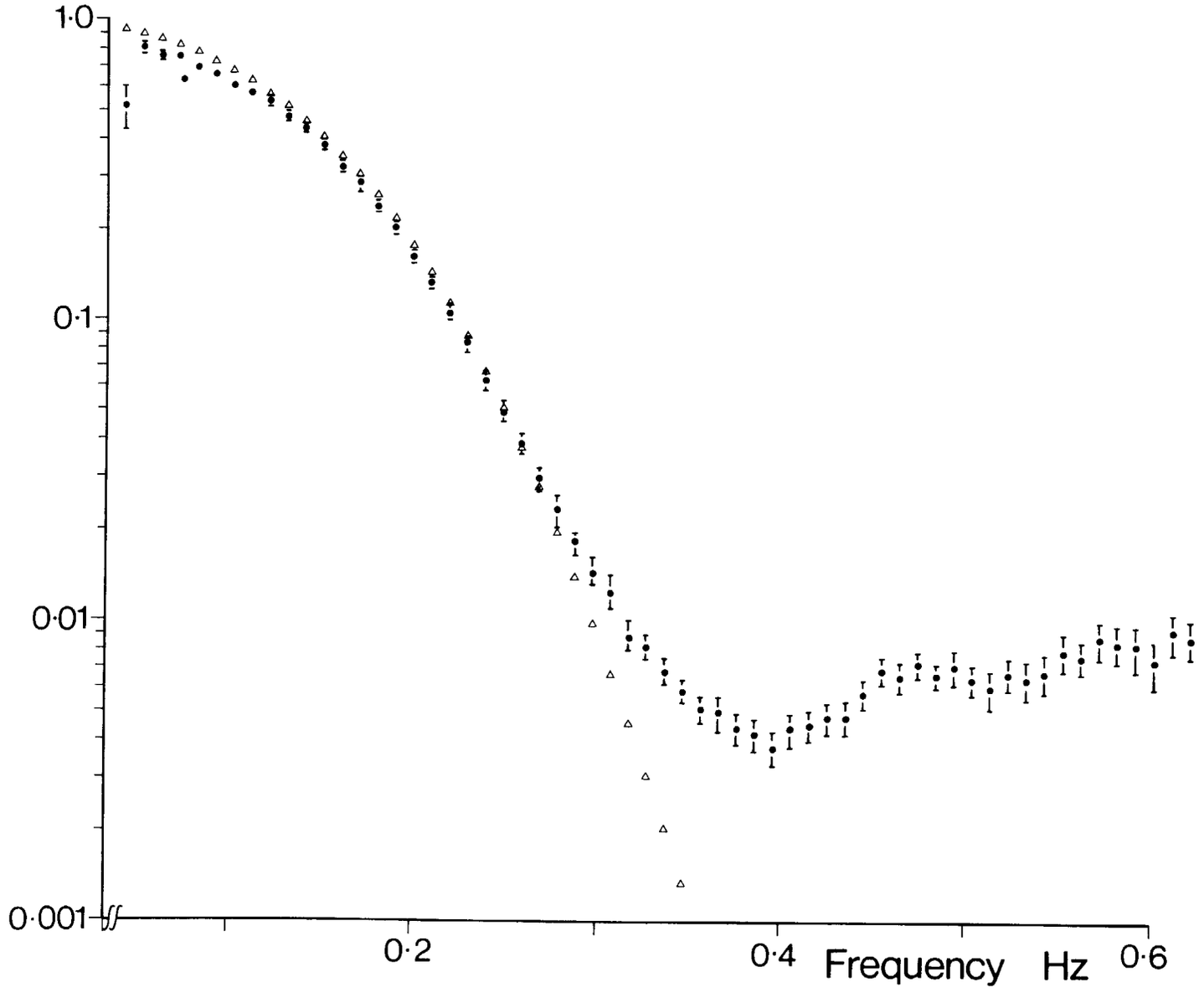

Figure 27 FM pressure recorder (uncorrected for attenuation with depth) .v. EMI laser. Slope, • , and 95% confidence interval on slope, I , of reduced major axis regression line (constrained through 0,0) fitted to the population of simultaneous spectral densities at each frequency. The form of the classical attenuation formula is indicated by the small triangles.

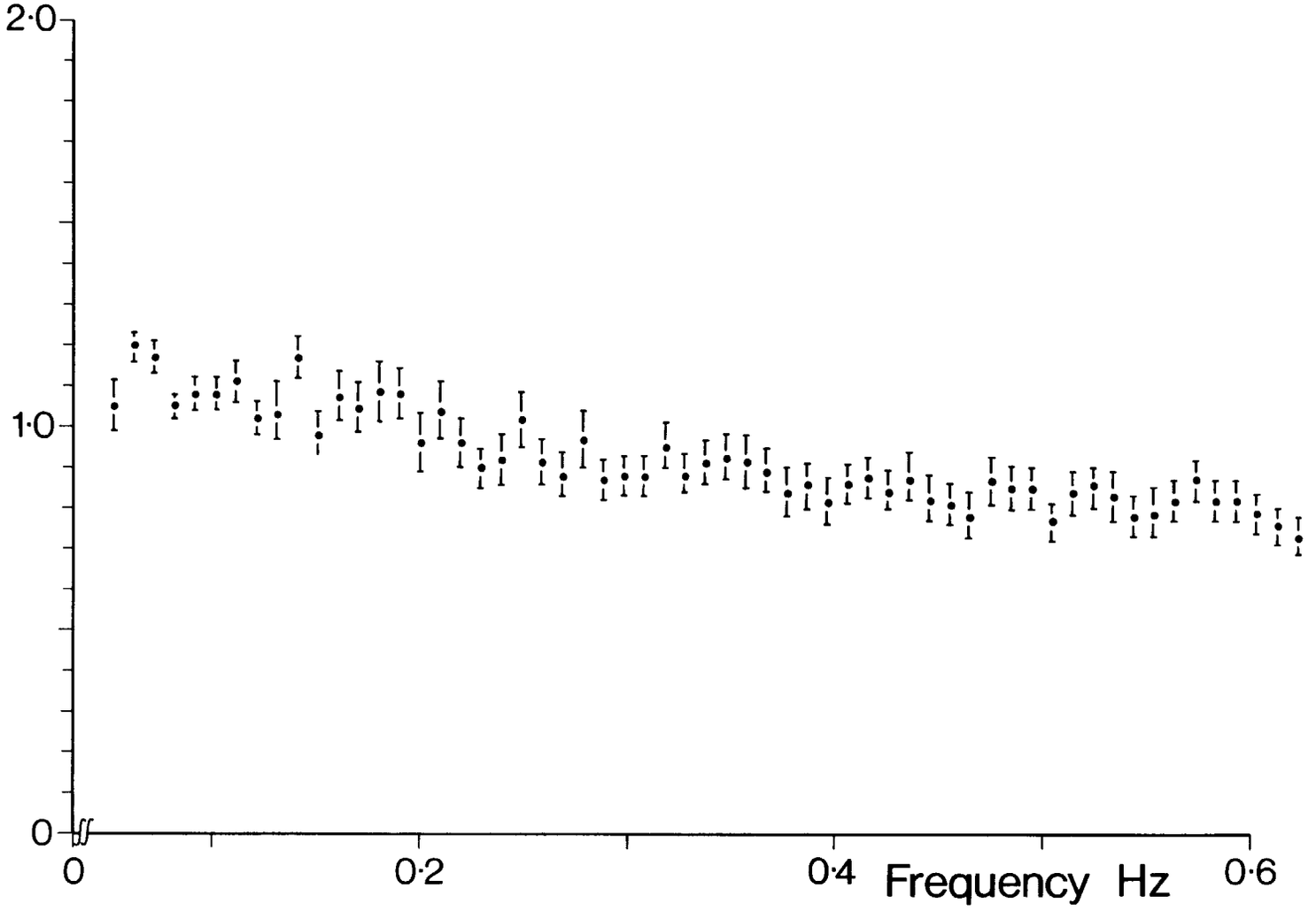

Figure 26 NBA Wavecrest .v. Datawell Waverider. Slope, • , and 95% confidence interval on slope, I , of reduced major axis regression line (constrained through 0,0) fitted to the population of simultaneous spectral densities at each frequency.

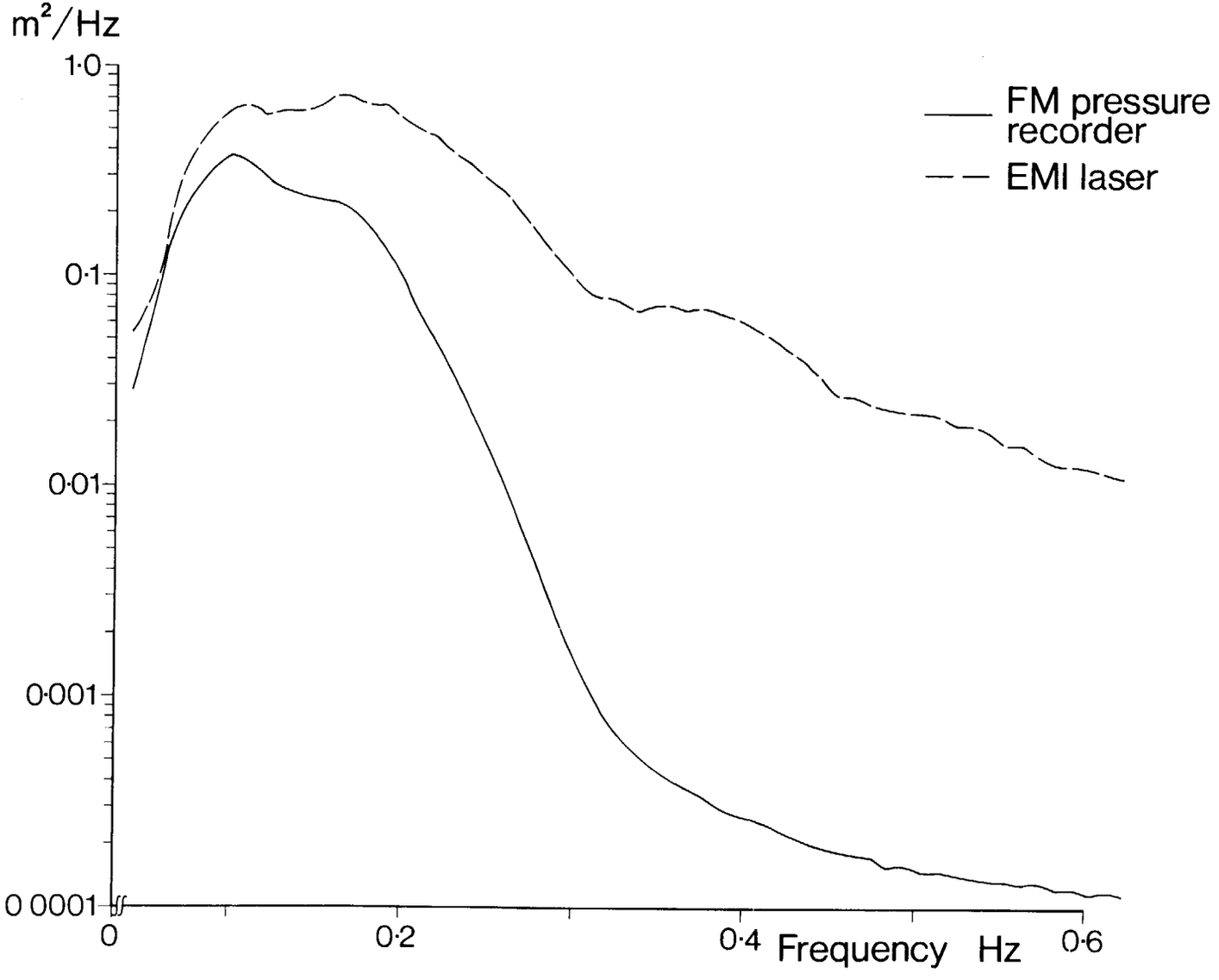

Figure 28 EMI laser and FM pressure recorder. Mean spectra derived from all valid records taken during the four day period of detailed comparison.

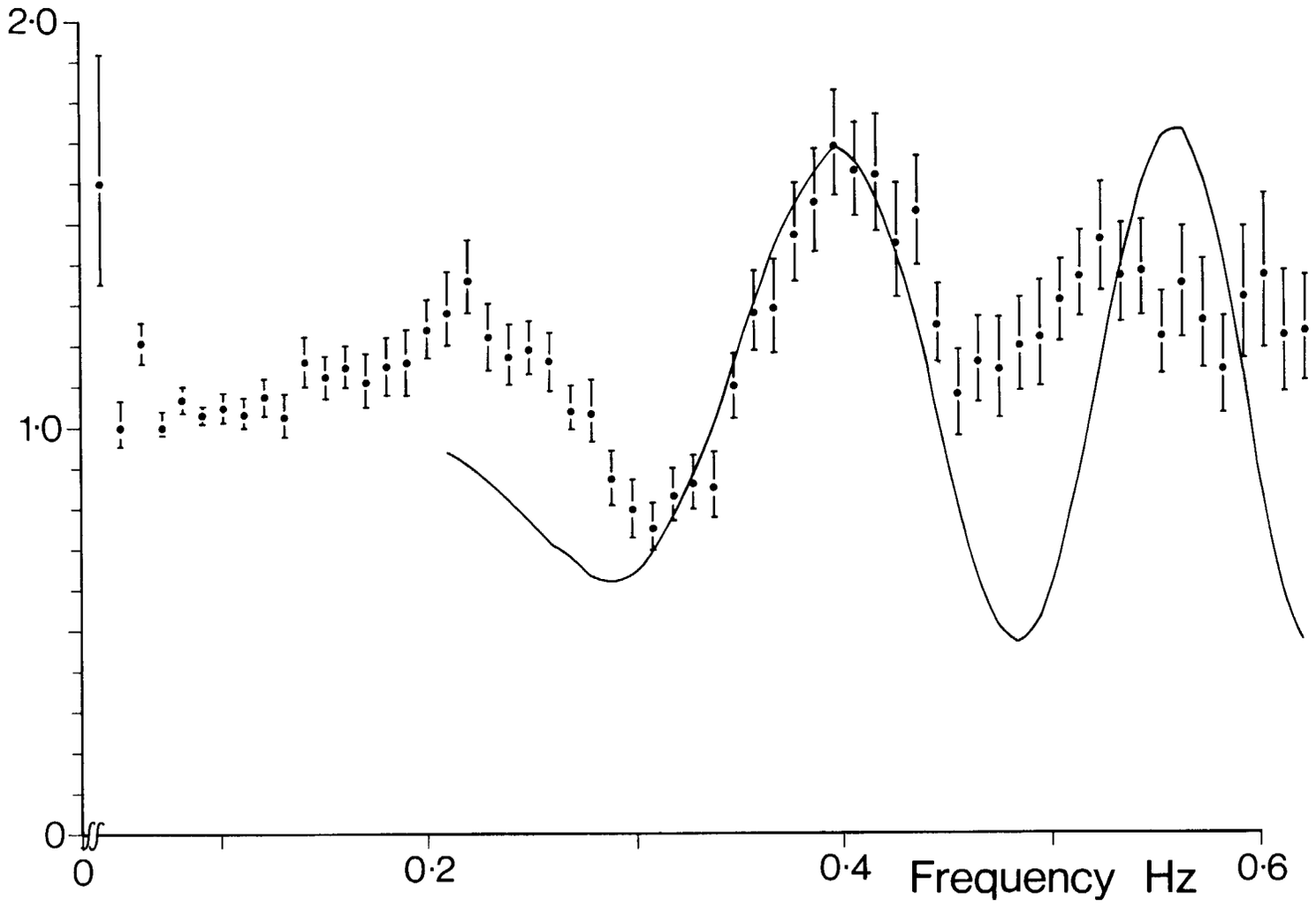

Figure 29 Ratio of variances in each frequency band of waves in the vicinity of the structure, and thus affected by partial reflection from the tower leg, to those in the distant field. Superimposed on the spectral density comparisons of figure 23.

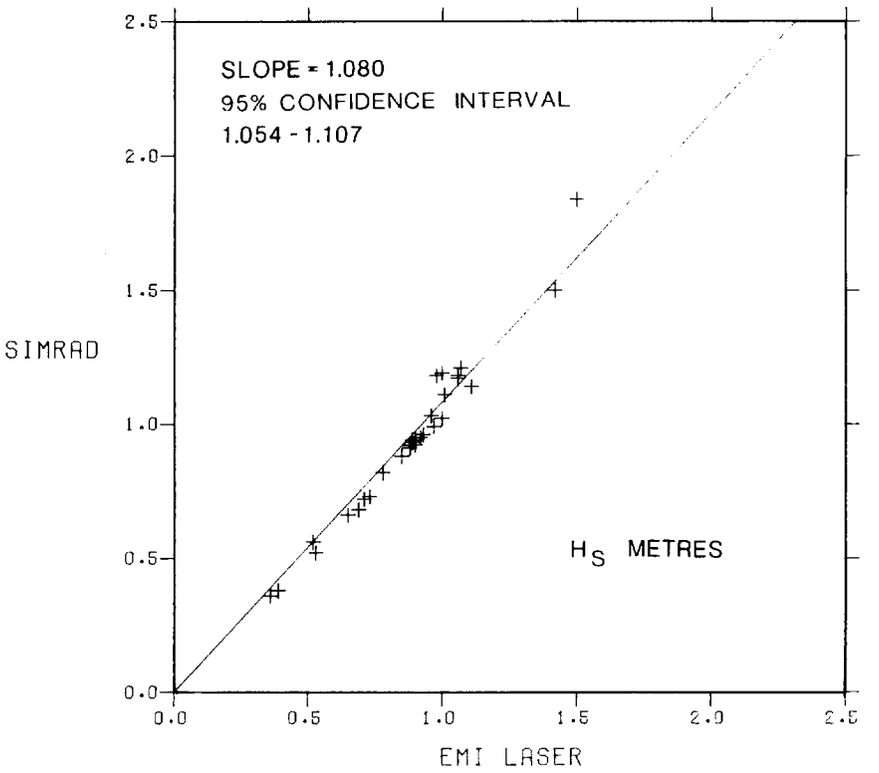

Figure 30a SIMRAD echo sounder .v. EMI laser. Comparison of significant wave height.

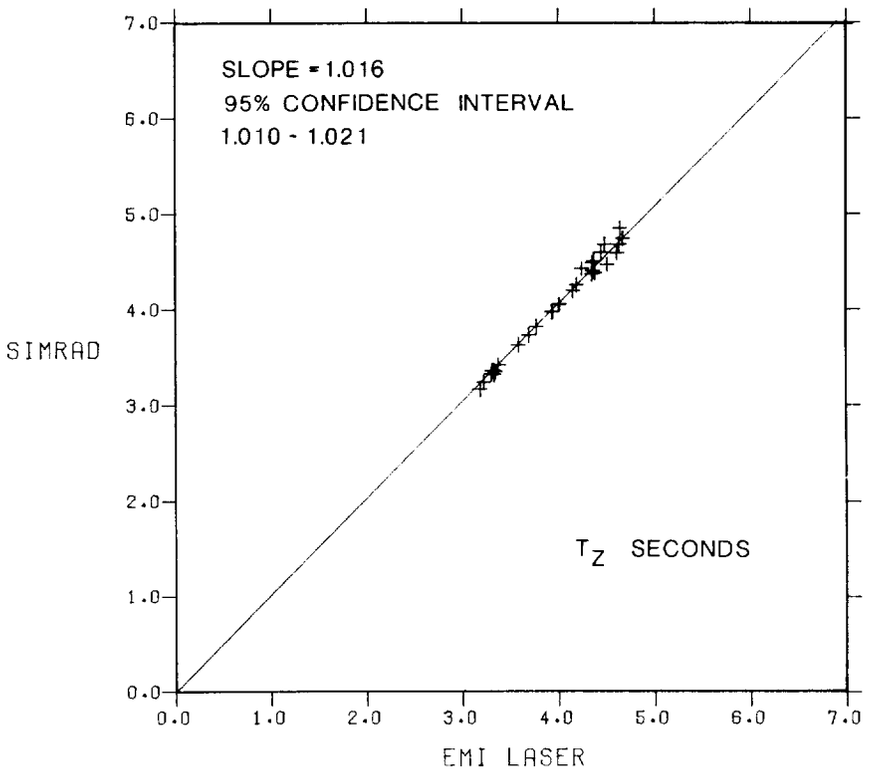

Figure 30b SIMRAD echo sounder .v. EMI laser. Comparison of mean zero crossing period.

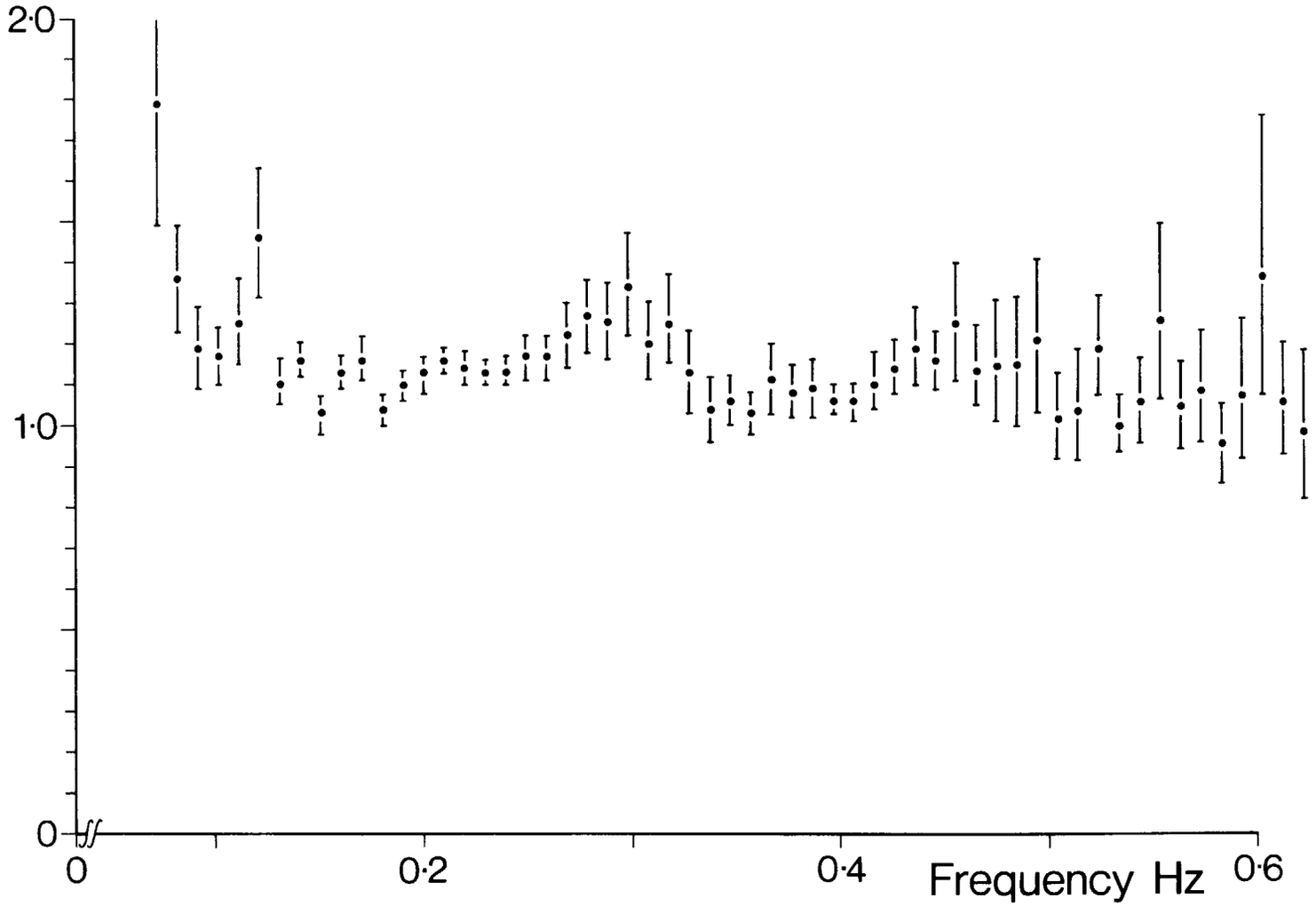

Figure 31 SIMRAD echo sounder .v. EMI laser. Slope, • , and 95% confidence interval on slope, I , of reduced major axis regression line (constrained through 0,0) fitted to the population of simultaneous spectral densities at each frequency.

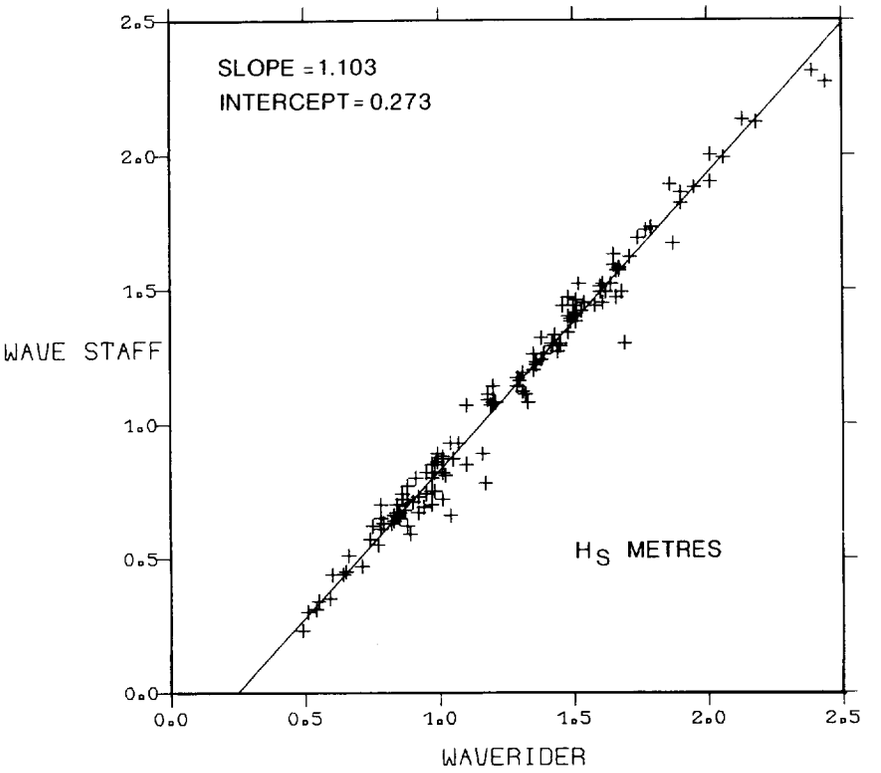

Figure 32 COMEX wave staff .v. Datawell Waverider. Comparison of significant wave height.

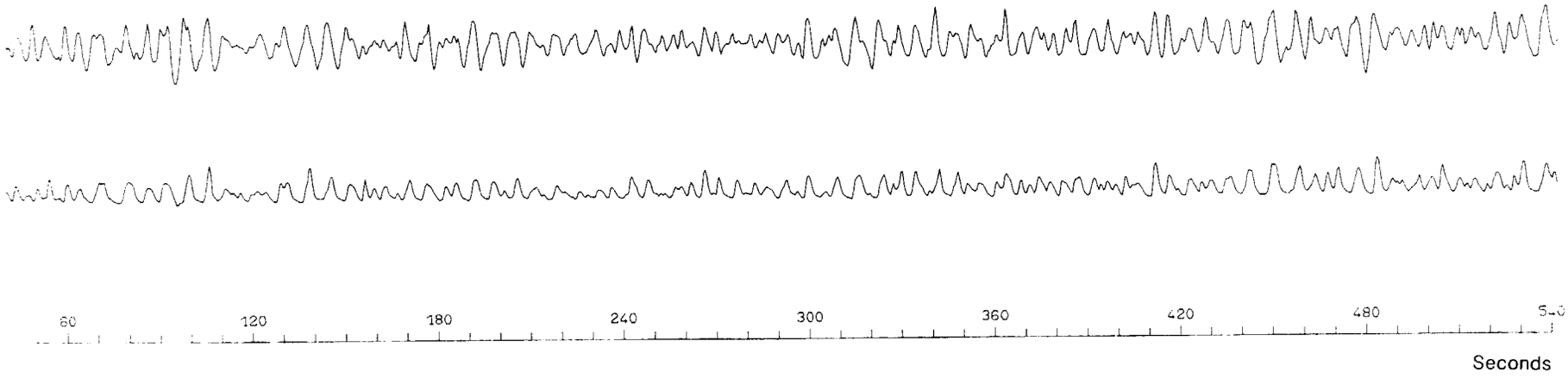

Figure 33 Example of faulty trace returned by COMEX wave staff (lower trace), with waves recorded simultaneously by the EMI laser for comparison.

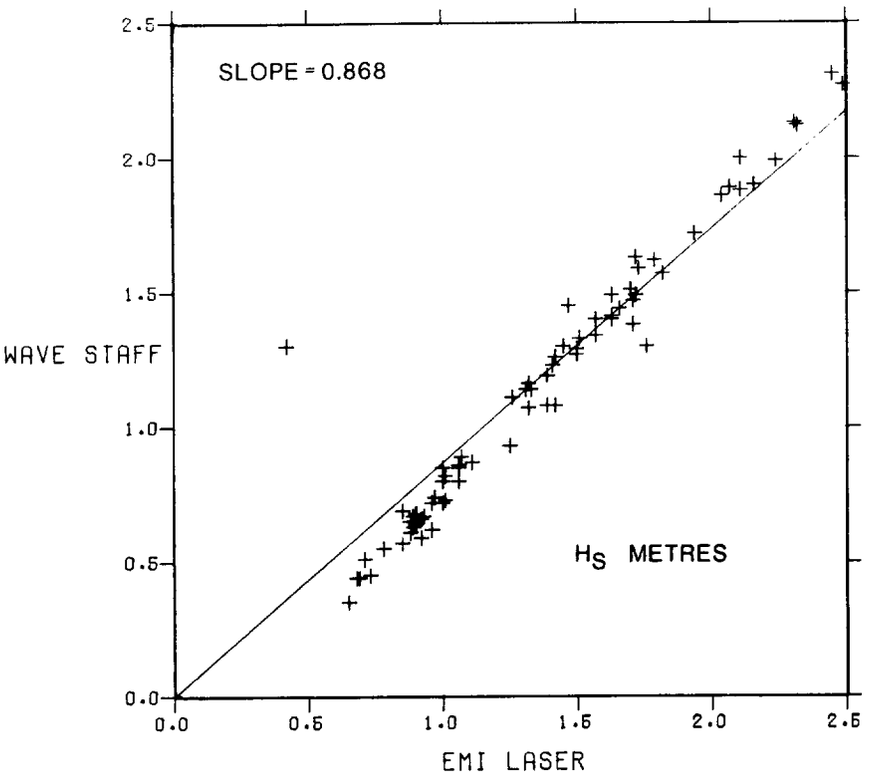

Figure 34a COMEX wave staff .v. EMI laser. Comparison of significant wave height.

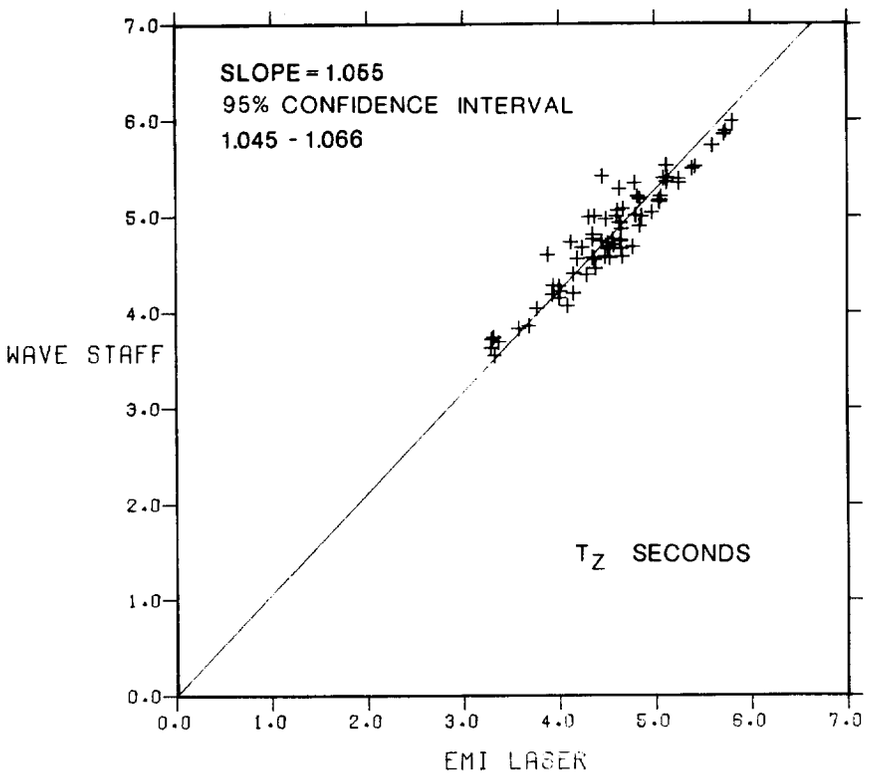

Figure 34b COMEX wave staff .v. EMI laser. Comparison of mean zero crossing period.

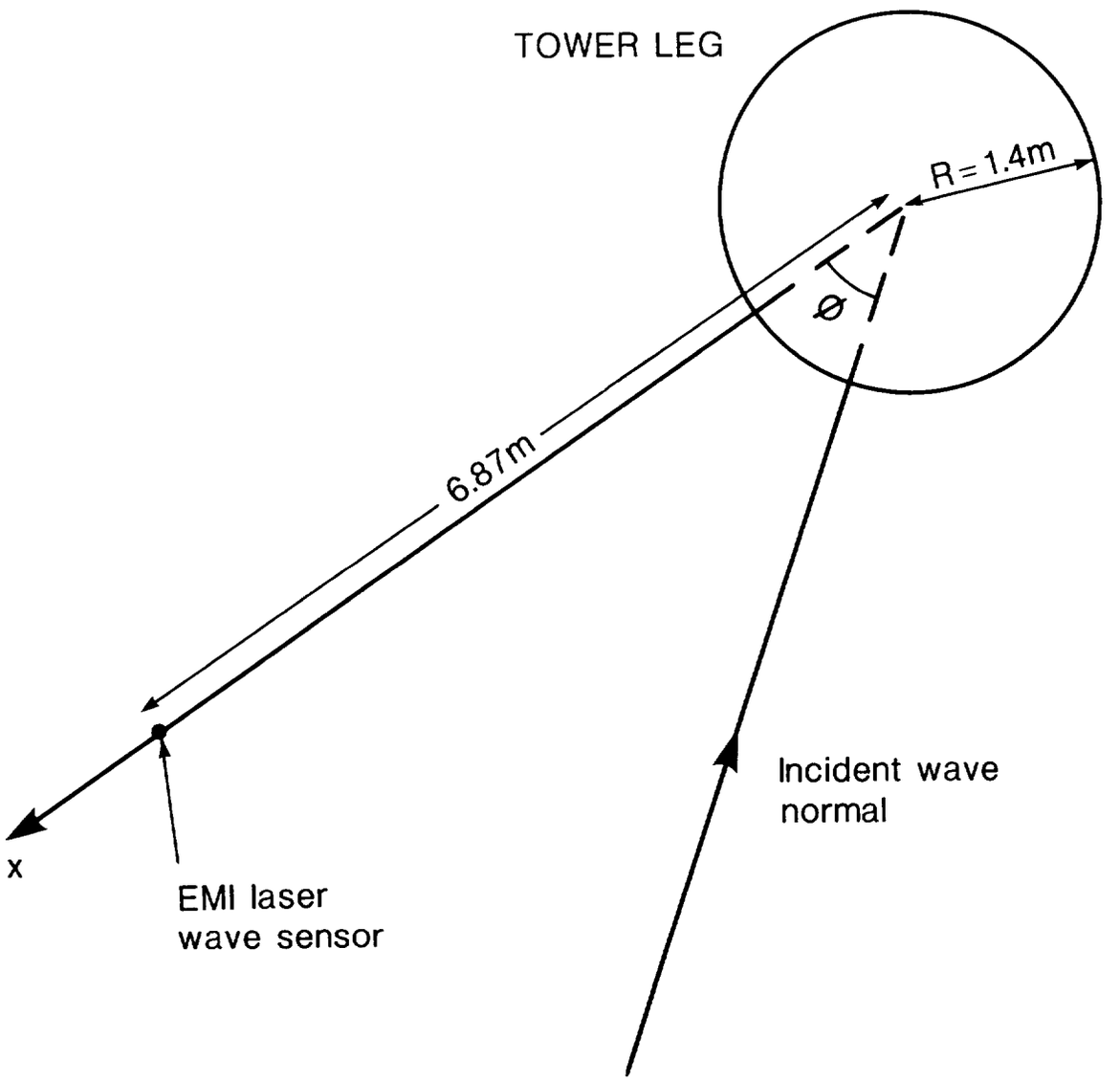

Fig 35 Geometry used in calculating the effect of wave reflections on the local wave climate.

9. REFERENCES

1. PITT, E G, DRIVER, J S, EWING, J A, 1978 Some intercomparisons between wave recorders Institute of Oceanographic Sciences Report no 43

2. WHEATLEY, J H W, 1976 A British offshore research facility National Physical Laboratory Report no R148

3. BISHOP, J R, 1978 A description of the Christchurch Bay Wave Force project National Maritime Institute Report no R33

4. TARDIVEL, W F, PARKER, A G, BAIRD, A A, 1980 Details of a new wave height measuring buoy National Maritime Institute Report no R98

5. PARKER A G, 1982 Personal communication

6. HAINE, R A, 1982 A one-bit microprocessor controlled data acquisition system pp 1/1-1/5 in Microprocessors in the Marine Industry, Colloquium held by the Institution of Electrical Engineers, London 16 April 1982 Digest no 1982/38

7. GREGORY, V, DELLARDE, B, 1977 MC 14500 B Industrial Control Handbook Motorora Semiconductor Products Inc, pp 106

8. V d VINGT, A J M, BOOT, J L J, DUIREVELD, A A, 1982 Intercomparisons of a SAAB radar, Syminex radar, EMI laser and a step gauge wave height meter Rijkswaterstaat, Netherlands

9. V d FLUGT, Ir A J M, 1982 Comparison of an improved EMI laser waveheight sensor and two step gauges Rijkwaterstaat, Netherlands

10. DRAPER, L, 1957 Attenuation of sea waves with depth La Houille Blanche no 6 Dec 1957 pp 1-6

11. WEIGEL, R L, 1964 P 26 in Oceanographical Engineering Englewood Cliffs, NJ Prentice-Hall

12. LONGUET-HIGGINS, M J and CARTWRIGHT, D E, 1957 The amplitude of waves reflected from a vertical circular cylinder NIO Internal Report A9

10. ACKNOWLEDGEMENTS

The authors would like to express their appreciation to the various people who have contributed to this work. In particular, they would like to mention: Dr A G Parker, Mr G W Pearce and Mr W F Tardivel of NMI and Mr R Cuffe of Valeport Developments (late of NMI), all of whom gave assistance with the siting, installation and maintenance of the equipment at the tower and shore station.

Mr I Storvik of Simrad, Mr W B Andrews of EMI, Mr R F Scrivens and Mr J Wardle of W S Ocean Systems (late of NBA) who made equipment available and gave advice on the deployment.

Many colleagues at IOS, especially Dr G N Crisp and Mr D E C Whiteway for their advice and assistance in devising and implementing the data analysis suite, Mr P M Hooper for assistance in installing and maintaining the equipment, and Dr A G Davies for the helpful discussions on the attenuation of surface waves, and Mrs C Kemp for the illustration and drawings.